ORGANOMETALLICS
Article
Cite This: Organometallics XXXX, XXX, XXX−XXX
pubs.acs.org/Organometallics

Regioselective Palladium-Catalyzed Heterocyclization−Sonogashira Coupling Cascades from 2-Alkynylbenzamides and Terminal Alkynes: Experimental and DFT Studies

Francisco Cruz,[†] Belén Vaz,[†] Unai Vilar,[‡] Aitor Ortega,[‡] Youssef Madich,[‡] Rosana Álvarez,*[,†] and José M. Aurrecoechea*[,‡]

[†]Departamento de Química Orgánica, Facultad de Química, Universidade de Vigo, CINBIO and IIS Galicia Sur, Campus As Lagoas-Marcosende, 36310 Vigo, Spain

[‡]Departamento de Química Orgánica II, Facultad de Ciencia y Tecnología, Universidad del País Vasco UPV/EHU, Apartado 644, 48080 Bilbao, Spain

Supporting Information

ABSTRACT: A regioselective heterocyclization−Sonogashira coupling cascade between 2-alkynylbenzamides and terminal alkynes is described. The reaction proceeds under Pd(II) catalysis, with air used as a terminal oxidant to regenerate the catalyst from the Pd(0) produced in the C−C coupling. The cascade process provides alkynyl-substituted isobenzofuranimine products in a single operation. These products are the result of a 5-exo O-cyclization, while products derived from the alternative 6-endo cyclization mode are observed in minor amounts. Two competing mechanisms have been considered to account for the observed results. Both involve heterocyclization, alkyne C−H activation, and reductive elimination steps but differ in the relative order of the first two. Control experiments using a preformed alkynylpalladium complex have shown that a mechanism starting with alkyne C−H activation is viable. On the other hand, DFT calculations indicate that the alternative cyclization-first mechanism is also competitive, particularly when PPh_3 is used as ligand. Calculations also suggest that the exo cyclization is favored over the endo mode by the presence of PPh_3 and σ-C Pd ligands in the activated complex undergoing cyclization.

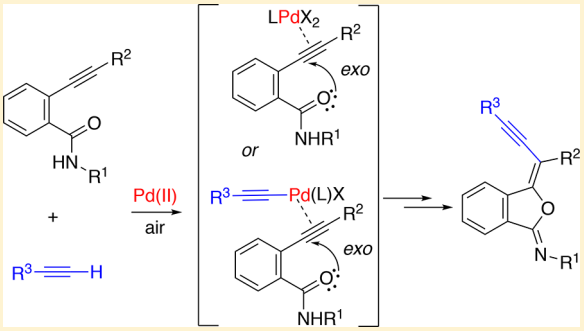

INTRODUCTION

The C−C triple bond is a versatile functionality with a rich reactivity profile, and as a result, alkynes are involved in a variety of useful synthetic transformations.[1] One of the most utilized approaches for the incorporation of alkynyl moieties into organic substrates is the metalation of the relatively acidic C_{sp}−H bond, as found in the classical Sonogashira-type reactions where a vinyl or aryl halide is coupled to a terminal alkyne, typically under Cu(I)/Pd(0)-catalyzed conditions (Scheme 1a).[2] Alternative methods have also been developed for alkyne coupling, which avoid the need for a halide precursor or for a Cu cocatalyst. Thus, under Pd-catalyzed conditions, terminal alkynes have undergone conjugate addition to α,β-unsaturated carbonyl derivatives,[3−6] cross-addition to ynol ethers,[7] and oxidative C_{sp2}−C_{sp} coupling.[8−15] In a broader synthetic context, the general field of metal-catalyzed heterocyclization−coupling reactions (Scheme 1b)[16] has been the subject of continuing attention because it provides access to functionalized heterocyclic structures with useful applications. The particular case of palladium-catalyzed heterocyclization−alkynylation cascades (Scheme 1c) is also known,[17−26] but it has received comparatively little attention despite its potential for the incorporation of alkynyl groups onto heterocyclic frameworks.

Scheme 1. Applications of Alkyne C−H Metalation

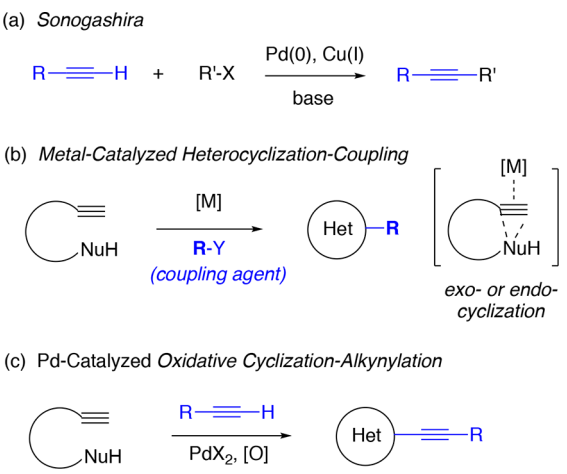

Received: July 24, 2018

DOI: 10.1021/acs.organomet.8b00519
Organometallics XXXX, XXX, XXX−XXX

One representative example of palladium-catalyzed heterocyclization−coupling is provided by the reactions of 2-alkynylbenzamides. These substrates have been shown to undergo palladium-catalyzed O-cyclization−coupling reactions with aryl[27] and allyl[28] halides, alkenes,[29−33] carbon monoxide,[34] and 2-alkynyldimethylanilines,[35] as well as oxidative homocoupling,[36] in all cases with good control of the regiochemistry (exo/endo) of cyclization (Scheme 2).

Scheme 2. Palladium-Catalyzed C−C Couplings of Alkynylbenzamides[a]

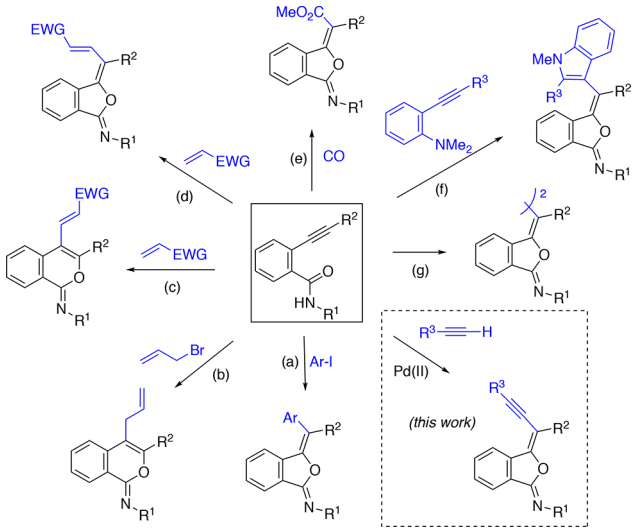

[a]Conditions: (a) $Pd(PPh_3)_4$, 2,6-lutidine, MeCN, reflux, Ar;[27] (b) $Pd_2(dba)_3$, DIPEA, toluene, 120 °C, Ar;[28] (c) $PdCl_2(PPh_3)_2$, KI, DMF, air, 80 °C;[29−31] (d) $Pd(OAc)_2$, PPh_3, KI, DMAP, DMF, air, 35 °C;[32] (e) PdI_2, KI, MeOH;[34] (f) $Pd(OAc)_2$, $Cu(OAc)_2$, nBu$_4$NI, HOAc, DMSO, air, 80 °C;[35] (g) $Pd(OAc)_2$, $Cu(OAc)_2$, K_2CO_3, MeCN, air, 100 °C.[36]

In the particular cases of the Pd(0)-catalyzed arylation- and allylation-type couplings (Scheme 2, conditions a and b), some insight into the reasons for the observed regiochemical tendencies has been provided through DFT calculations,[28] but for the rest of the reported alkynylbenzamide reactions of Scheme 2 a rationalization of the observed regiochemistries is still lacking. We have targeted the related cascade reactions between alkynylbenzamides and terminal alkynes as a new extension of the range of applications of alkynylbenzamides, while also aiming at providing further information on the general issue of the regioselectivity of cyclization. We now report the preparation of alkynylated isobenzofuranimine derivatives[37] from alkynylbenzamides and terminal alkynes, under Pd(II)-catalyzed oxidative conditions (Scheme 2, box). Additionally, we have also studied this reaction computationally as a means to provide a possible rationalization for their experimentally observed 5-exo-cyclization regiochemical preference.

■ RESULTS AND DISCUSSION

Preparation of Alkynylated Isobenzofuranimines. Reaction conditions were surveyed using alkynylbenzamide **1a** and phenylacetylene (**2a**) as model substrates (Table 1). In all cases, the isobenzofuranimine derivative **3a**, derived from a 5-exo O-cyclization, was the major product, while the corresponding six-membered-ring isomer **4a** was obtained in minor amounts. Using $Pd(OAc)_2$ as catalyst, a tendency toward an increasing **3a**/**4a** ratio with a decreasing reaction temperature was observed (entries 1−4). However, for practical purposes, the reaction was too slow at room temperature, with some starting material being recovered even after prolonged reaction times (5% recovery of starting **1a** after 33 h, entry 4). The formation of the diylidenebisisobenzofuranimine **5a**,[32] devoid of the moiety derived from the terminal alkyne, was also observed. The likely origin of this product is the competing oxidative dimerization of the starting benzamide, a process previously reported in the $Pd(OAc)_2$-catalyzed reactions of alkynylbenzamides under oxidative conditions (Scheme 2, conditions g).[36] In line with this precedent, **5a** was generally observed as a byproduct in the entries of Table 1 featuring $Pd(OAc)_2$ as catalyst but was absent with other catalysts (entries 10 and 11). The formation of **5a** became the major outcome of the reaction with the use of a catalytic amount of CuI, an additive intended as a cocatalyst in the Sonogashira-type step of the cyclization−coupling process (entry 5). In a control experiment, **5a** was the only observed product when the reaction was run in the absence of a terminal alkyne (entry 6). The exo/endo regioselectivity improved with the addition of NaOAc (entries 7 and 8) or K_2CO_3 (entry 9) but (especially in the later case) at the expense of increasing the extent of formation of **5a**. The regiochemical preference for a 5-exo cyclization was maintained with the use of $PdCl_2(PPh_3)_2$ (entry 10) and $Pd(TFA)_2$ (entry 11) as catalysts, but yields and selectivity were lower relative to the $Pd(OAc)_2$-catalyzed reactions. Furthermore, while $Pd(OAc)_2$ promoted an efficient reaction at 35 °C, those two catalysts required higher temperatures, especially $PdCl_2(PPh_3)_2$. The effect of the phosphine ligand was also briefly examined (entries 12−16). As shown by entries 12−14, the tendency toward an exo-selective process is independent of the presence or absence of a phosphine ligand but the use of PPh_3 is needed for useful reactivity (entry 12 vs entry 3). However, either increasing or decreasing its electron-donating ability led to inferior results (entries 12−14). Furthermore, when the reaction progress was followed by GC-MS (see the Supporting Information), it was observed that the reaction product was not detectable until the free PPh_3 present in the medium had been substantially oxidized to the corresponding phosphine oxide $OPPh_3$ (1.5 h). At that point, a diyne product evolving from the oxidative dimerization of alkyne **2a** had also begun to form. This apparent induction period disappeared when a combination of PPh_3 (5 mol %) and $OPPh_3$ (5 mol %) was used instead of the customary 10 mol % of PPh_3, and the reaction was still effective under those conditions (entry 15). In comparison, the use of a reduced amount of PPh_3 (5 mol %) without $OPPh_3$ was less effective (entry 16), and $OPPh_3$ alone led to a very slow reaction (entry 17). These phosphine and phosphine oxide effects could indicate that the stabilizing role of the ligands needs to be combined with a relative lability in one of them ($OPPh_3$),[38] probably to facilitate the availability of a vacant position at palladium for coordination of either one of the alkyne reagents.[39]

Next, the study of the heterocyclization−alkynylation reaction was extended to other substrates, and the corresponding results are presented in Table 2. While the conditions of entry 3 of Table 1 were used as a standard, occasionally the addition of NaOAc (0.1 equiv, conditions of entry 7 of Table 1) was found advantageous in cases where yields were unusually low using the standard conditions (Table 2, entries

DOI: 10.1021/acs.organomet.8b00519
Organometallics XXXX, XXX, XXX−XXX

Table 1. Survey of Reaction Conditions for Heterocyclization−Alkynylation[a]

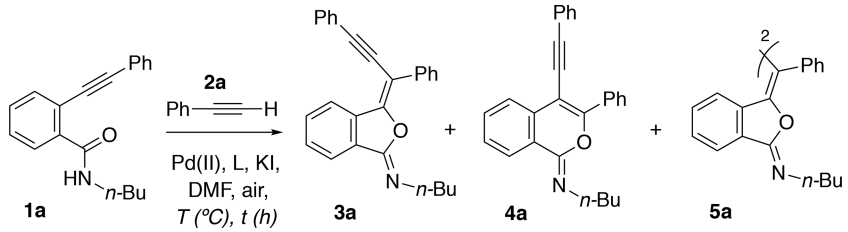

entry	Pd(II), L, additive	T (°C)	t (h)	**3a** (%)[b]	**4a** (%)[b]	crude **3a**/**4a**	**5a** (%)[b]
1	$Pd(OAc)_2$, PPh_3	80	6	36	10	3.6	9
2	$Pd(OAc)_2$, PPh_3	50	8	64	8	8.0	12
3	$Pd(OAc)_2$, PPh_3	35	15	69 (63)[c]	4 (3)[c]	17.2	5(5)
4[d]	$Pd(OAc)_2$, PPh_3	25	33	66	4	16.5	3
5[d]	$Pd(OAc)_2$, PPh_3, CuI (0.1)	35	15	11	2	5.5	29
6[e]	$Pd(OAc)_2$, PPh_3	80	6				69
7	$Pd(OAc)_2$, PPh_3, NaOAc (0.1)	35	7	73	3	24	6
8	$Pd(OAc)_2$, PPh_3, NaOAc (0.5)	35	15	61	2	30	8
9	$Pd(OAc)_2$, PPh_3, K_2CO_3 (0.1)	35	15	46	2	23	24
10	$PdCl_2(PPh_3)_2$	80	7	42	10	4.2	
11[d]	$Pd(TFA)_2$, PPh_3	50	41	20	7	3.0	
12[d]	$Pd(OAc)_2$	35	15	39	3	13	3
13[d]	$Pd(OAc)_2$, $P[(p\text{-MeO})C_6H_4]_3$	35	15	41	8	5.1	
14[d]	$Pd(OAc)_2$, $P[(p\text{-}CF_3)C_6H_4]_3$	35	15	59	4	14.7	8
15	$Pd(OAc)_2$, PPh_3,[f] $OPPh_3$[f]	35	7	76	5	15.2	6
16	$Pd(OAc)_2$, PPh_3[f]	35	15	52	3	17	4
17[d]	$Pd(OAc)_2$, $OPPh_3$[g]	35	15	11	1	11	2

[a]Relative amounts of reagents unless otherwise indicated: phenylacetylene (2 equiv), Pd complex (5 mol %), phosphine ligand (10 mol %), KI (0.5 equiv), additive (number of equivalents as indicated). [b]Crude yields determined by ^{1}H NMR integration using an internal standard. [c]Isolated yield. [d]Starting material **1a** was recovered (5% in entry 4, 38% in entry 5, 40% in entry 11, 33% in entry 12, 27% in entry 13, 13% in entry 14, 60% in entry 17). [e]Alkyne **2a** was omitted. [f]5 mol %. [g]10 mol %.

Table 2. Preparation of Alkynylisobenzofuranimines 3 from Alkynylbenzamides 1 and Alkynes 2.[a]

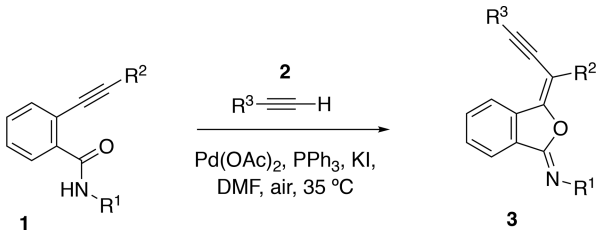

	1	R^1	R^2	R^3	conditions	t (h)	**3**	yield (%)[b]
1	**1a**	*n*-Bu	Ph	Ph	A	15	**3a**[c]	63
2	**1b**	*n*-Bu	$(p\text{-MeO})C_6H_4$	cyclohexenyl	B	15	**3b**	58
3	**1c**	*n*-Bu	$(p\text{-}CO_2Me)C_6H_4$	$(p\text{-MeO})C_6H_4$	A	20	**3c**	68
4	**1c**	*n*-Bu	$(p\text{-}CO_2Me)C_6H_4$	cyclohexenyl	A	20	**3d**[d]	63
5	**1c**	*n*-Bu	$(p\text{-}CO_2Me)C_6H_4$	Ph	B	6	**3e**	60
6	**1d**	Ph	$(p\text{-MeO})C_6H_4$	$(p\text{-MeO})C_6H_4$	A	20	**3f**	53
7	**1d**	Ph	$(p\text{-MeO})C_6H_4$	3-thienyl	A	20	**3g**	49
8	**1e**	Ph	Ph	Ph	A	22	**3h**	45
9	**1f**	$(p\text{-MeO})C_6H_4$	*n*-Hex	Ph	B	6	**3i**	57
10	**1a**	*n*-Bu	Ph	n-Hex	A	23	**3j**	53
11	**1g**	CH_2Ph	Ph	Ph	A	16	**3k**	61
12	**1h**	$(p\text{-Cl})C_6H_4$	*n*-Hex	Ph	A	16	**3l**	69

[a]Conditions A: benzamide **1**, alkyne **2** (2 equiv), $Pd(OAc)_2$ (5 mol %), PPh_3 (10 mol %), KI (0.5 equiv) in DMF at 35 °C under an air atmosphere. Conditions B: as in conditions A with the addition of NaOAc (0.1 equiv). [b]Isolated yield (%). [c]Also isolated were **4a** (3%) and **5a** (5%). [d]Also isolated was **5d** (6%).

2, 5, and 9). Alternatively, the use of $OPPh_3$ as additive (conditions of entry 15 of Table 1) was also considered but, in addition to providing a lower exo/endo ratio, the yield advantage observed with **3a** proved not to be general with other substrates (see Table S1 in the Supporting Information). In any case, the preparation of isobenzofuranimines **3** by a

DOI: 10.1021/acs.organomet.8b00519
Organometallics XXXX, XXX, XXX−XXX

cyclization–alkynylation process was successful with a variety of combinations of *o*-alkynylbenzamides **1** and terminal alkynes **2**. As shown in Table 2, useful benzamides **1** may contain either alkyl or aryl groups at R^1 and R^2 and, additionally, substitution at the aryl groups with ED and EW groups was well tolerated. In turn, participating terminal alkynes **2** include examples where the substituent R^3 is alkyl, alkenyl, aryl, or heteroaryl. In the case of aryl substitution, an ED group again provided useful results but the incorporation of the EW CO_2Me group resulted in lack of reactivity, with recovery of the starting benzamide. In all cases, the regiochemistry of cyclization was very predominantly exo. Signals associated (by analogy with **4a**) to isomers derived from a 6-endo cyclization were sometimes observed in the ^{1}H NMR spectra of the crude products but always in minor amounts. In general, yields were only moderate but, because of its simplicity, this one-step procedure is a practical alternative to a reported two-step strategy using the iodocyclization of an alkynylbenzamide followed by a traditional palladium-catalyzed Sonogashira cross-coupling.[37b,d,40]

Mechanism of Cyclization–Alkynylation. Mechanistically, we interpret this transformation in terms of a Pd(II)-induced oxycyclization followed by alkynylative C–C bond formation (Scheme 3), where an additional alkyne C_{sp}–H

Scheme 3. Pathways for Palladium-Catalyzed Heterocyclization–Alkynylation: (A) Cyclization First Pathway; (B) C–H Palladation First Pathway

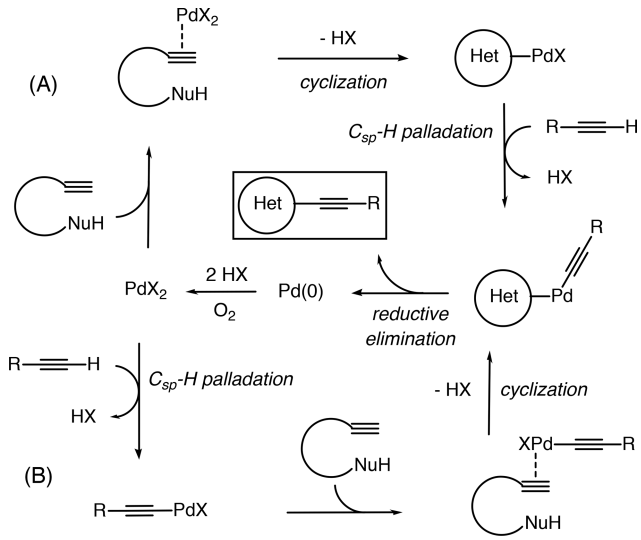

palladation step, leading to a σ-alkynylpalladium complex, has been incorporated into the general idea represented in Scheme 1b. Two pathways are then possible depending on whether alkyne C–H palladation precedes or follows the heterocyclization event. For example, pathway A, where cyclization precedes the C–H palladation step, has been reported to be followed by the aminocyclization–alkynylation reactions of 2-alkynyldimethylaniline derivatives,[19] whereas pathway B would be reminiscent of the mechanism followed by typical Pd(0)-catalyzed reactions such as arylations, where the initial oxidative addition of an aryl halide provides the Pd(II) species needed to activate the C–C triple bond and trigger heterocyclization.[16b,d–f,41,42] Interestingly, we have recently found that, in the particular case of arylations (and allylations) of 2-alkynylbenzamides, the final regiochemical outcome is partially determined by the character of the R group (aryl or allyl) in the organopalladium(II) RPdY σ complex intermediate.[28]

The formation of **5a** in the absence of a terminal alkyne (Table 1, entry 6) indicates that pathway A is operative, at least at the cyclization stage. We have tested the viability of pathway B with the control experiment shown in Scheme 4. Thus, when

Scheme 4. Control Reactions for Viability of Mechanism B

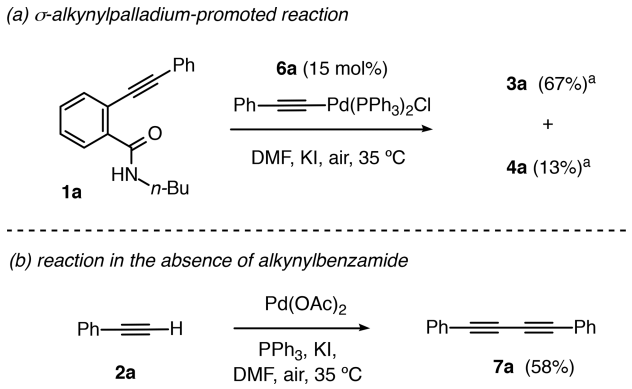

[a]Yield based on the starting amount of **6a**.

the preformed σ-alkynyl complex **6a**[43] was reacted with benzamide **1a** (Scheme 4a), the alkynylated products **3a** and **4a** were obtained in 80% overall yield in a ratio (**3a**/**4a** = 5/1) comparable to that found with the $PdCl_2(PPh_3)_2$ catalyst (Table 1, entry 10). This indicated that **6a** is indeed capable of promoting the alkynylbenzamide cyclization and eventually deliver the cross-coupling product **3** with the same exo selectivity as in the catalytic reaction. Additionally, alkyne **2a** was treated with $Pd(OAc)_2$ under the standard reaction conditions of entry 3 (Table 1) *in the absence of a benzamide 1* (Scheme 4b). This resulted in the consumption of **2a**, with formation of diyne **7a**,[44,45] showing that the alkyne C–H palladation (a necessary step in both mechanisms) is a relatively facile process under the standard alkynylation conditions. Diyne **7a** was not observed upon GC-MS monitoring of the reaction in Scheme 4a. Overall, without ruling out any other interpretation, the results shown in Scheme 4 support the viability of pathway B.

Computational Studies. We have used alkyne **2a** and the slightly simplified alkynylbenzamide **I** (where Me replaces the *n*-Bu group of **1a**) as model substrates for DFT calculations, where pathways A and B have been computed for a reaction promoted by $Pd(OAc)_2$ in the presence of the experimental ligand PPh_3. The corresponding energy profiles are displayed in Figures 1 and 2.

After an initial exergonic complexation (−36.2 kcal/mol) of $Pd(OAc)_2$ to benzamide **I** in the presence of PPh_3, cyclization takes place with relatively low activation energy (4.6 and 9.6 kcal/mol for exo and endo modes, respectively), and zwitterionic complexes **IIIPPh$_3$** are generated in an exergonic process (9.7 and 11.0 kcal/mol). From **IIIPPh$_3$**, phenylacetylene (**2a**) is incorporated with release of acetic acid and geometric isomerization, leading to alkyne complexes **IVPPh$_3$**. A facile C–H palladation of the terminal alkyne of **IVPPh$_3$** (activation energies 3.5 and 2.8 kcal/mol for exo and endo modes, respectively) then originates σ-alkynyl palladium complexes **VPPh$_3$**. The reductive elimination precursors **VIPPh$_3$** are then generated from **VPPh$_3$** upon release of an

DOI: 10.1021/acs.organomet.8b00519
Organometallics XXXX, XXX, XXX–XXX

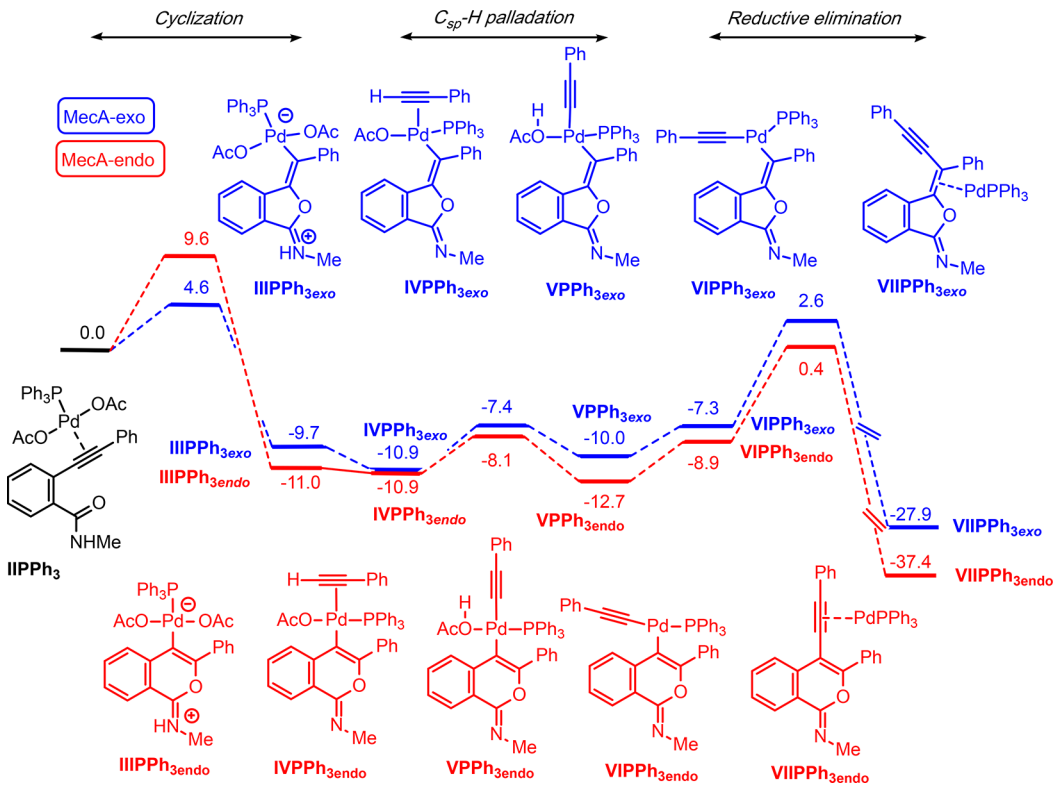

Figure 1. Reaction profile for pathway A in a reaction promoted by $Pd(OAc)_2/PPh_3$ (energy values in kcal/mol; wB97XD/LANL2DZ/6-31G*//wB97XD-SMD (DMF)/LANL2DZ/6-31G*).

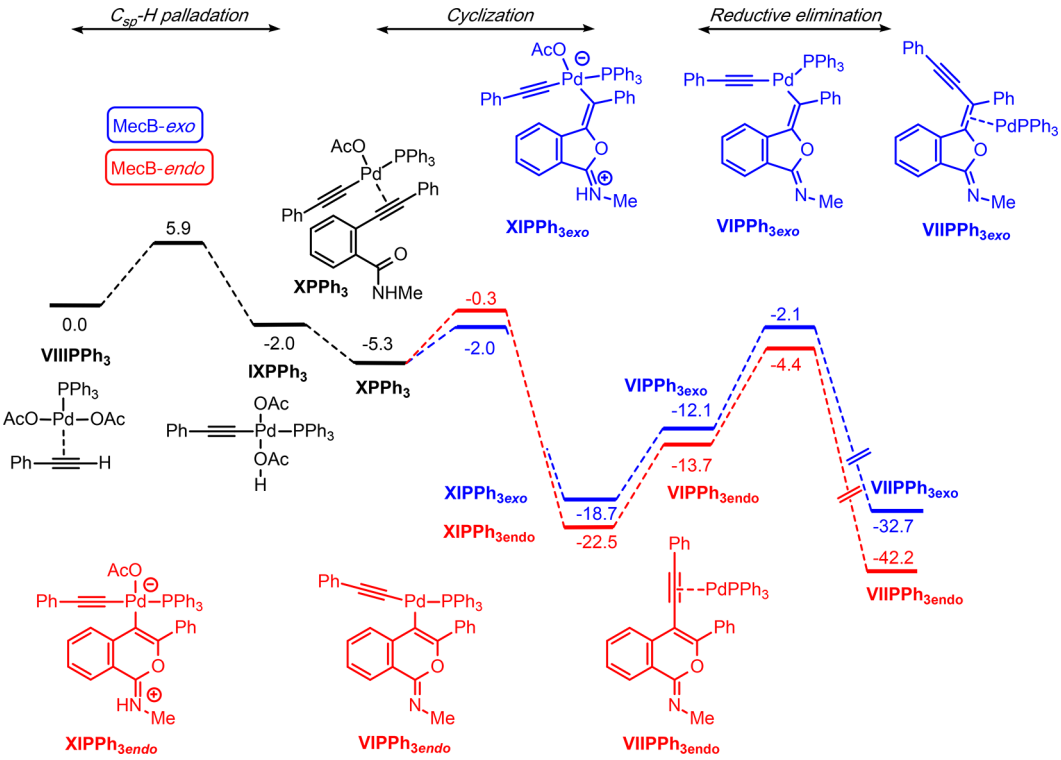

Figure 2. Reaction profile for pathway B in a reaction promoted by $Pd(OAc)_2/PPh_3$ (energy values in kcal/mol; wB97XD/LANL2DZ/6-31G*//wB97XD-SMD (DMF)/LANL2DZ/6-31G*).

acetic acid molecule and geometric isomerization. The final reductive elimination step is also a relatively low energy process (9.6 and 9.3 kcal/mol for exo and endo modes, respectively), leading to products **VII**.

Pathway B parallels pathway A in that the initial complexation of $Pd(OAc)_2$ to phenylacetylene (**2a**) in the presence of PPh_3 is also a strongly exergonic process (−31.4 kcal/mol), while C−H palladation of the terminal alkyne in the resulting

DOI: 10.1021/acs.organomet.8b00519
Organometallics XXXX, XXX, XXX−XXX

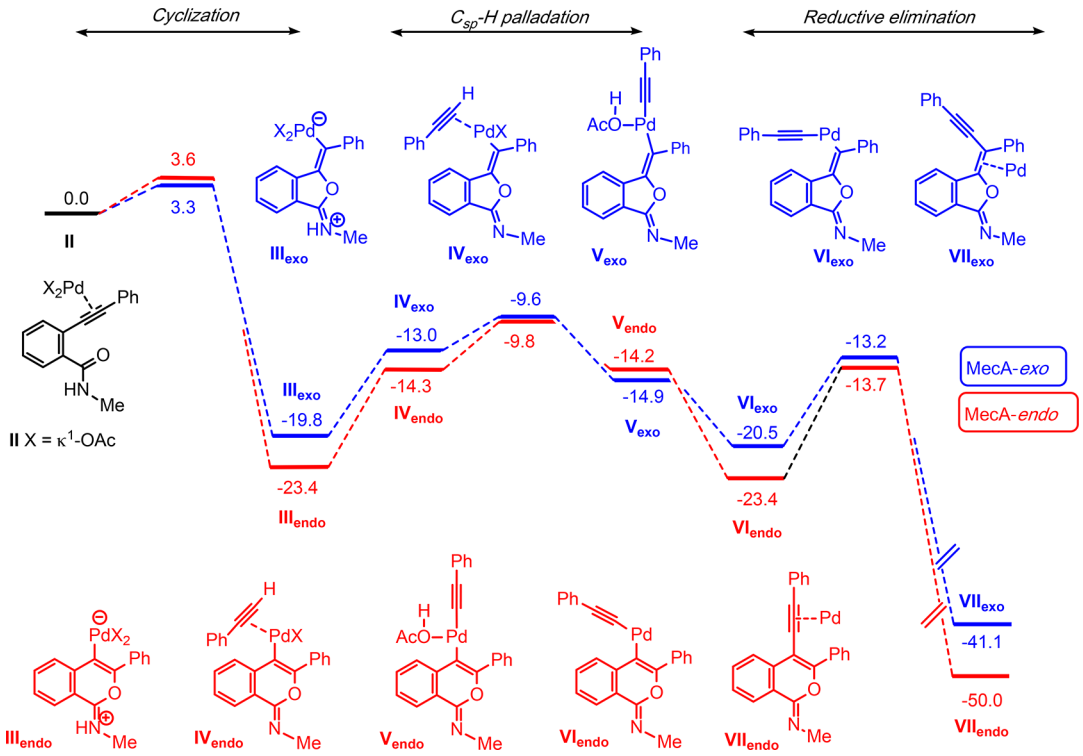

Figure 3. Reaction profile for pathway A in a reaction promoted by $Pd(OAc)_2$ in the absence of PPh_3 (energy values in kcal/mol; wB97XD/LANL2DZ/6-31G*//wB97XD-SMD (DMF)/LANL2DZ/6-31G*).

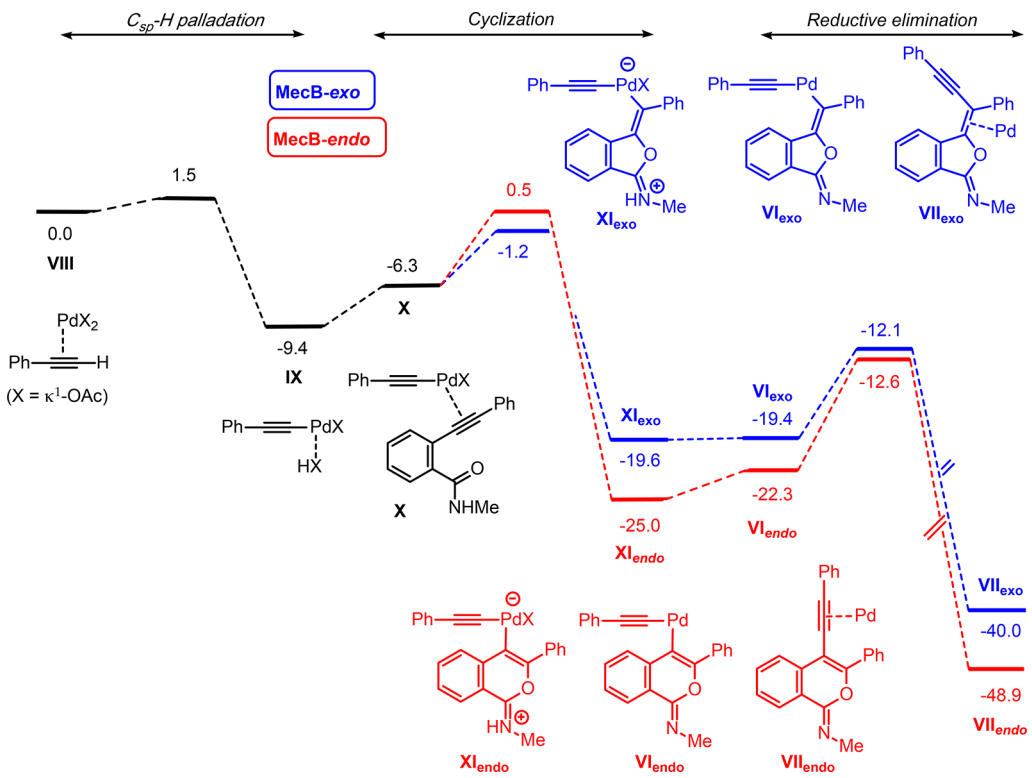

Figure 4. Reaction profile for pathway B in a reaction promoted by $Pd(OAc)_2$ in the absence of PPh_3 (energy values in kcal/mol; wB97XD/LANL2DZ/6-31G*//wB97XD-SMD (DMF)/LANL2DZ/6-31G*).

complex **VIIIPPh$_3$** is similarly facile (activation energy 5.9 kcal/mol), consistent with the previously reported low activation barriers (6−9 kcal/mol) also computed for alkyne C−H palladation using either a PhPdOH complex with assistance by nBuNH$_2$[46] or $Pd(OAc)_2/PMe_3$ as catalyst.[6] The resulting σ-alkynyl palladium complex **IXPPh$_3$** undergoes an exergonic (3.3 kcal/mol) ligand exchange with release of acetic acid and incorporation of alkynylbenzamide **I**, leading to the

DOI: 10.1021/acs.organomet.8b00519
Organometallics XXXX, XXX, XXX−XXX

cyclization precursor **XPPh$_3$**. Both cyclization modes have low activation energies (3.3 and 5.0 kcal/mol for exo and endo modes, respectively), and the formation of the cyclized σ complexes **XIPPh$_3$** is quite exergonic. Release of an acetic acid molecule from **XIPPh$_3$** then leads to the reductive elimination precursors **VIPPh$_3$**, where pathways A and B would converge.

The cyclization step is the point where both pathways, A and B, branch into competing endo and exo modes. Calculations predict fast and exergonic cyclizations in all cases, with large energy differences between the forward and backward activation barriers. Additionally, while the endo cyclization products are more stable than the exo products, these are formed with lower energy barriers. Because the cyclization reverse reactions have higher or very similar activation energies in comparison to the subsequent forward processes, calculations would predict an overall exo selectivity irrespective of the pathway (A or B) followed. The combined results presented in Figures 1 and 2 would suggest a competition between pathways A and B. Pathway A would have an initial driving force advantage since, according to calculations, coordination of Pd(OAc)$_2$ to the alkynylbenzamide is more favorable (by 4.8 kcal/mol) than that to the terminal alkyne. Additionally, pathway A proceeds through lower energy intermediates and with lower activation energies. As a result, pathway A would seem to be the preferred pathway under conditions using PPh$_3$ ligands.

As shown in Table 1 (entry 12) the exo selectivity is also experimentally maintained in the absence of phosphine ligands. We have modeled this alternative situation using Pd(OAc)$_2$ alone as reaction promoter. The resulting corresponding energy profiles for pathways A and B are displayed in Figures 3 and 4.

The geometries in Figures 3 and 4 tend to parallel those displayed in Figures 1 and 2, respectively, with a C−H agostic interaction (from the AcO Me group) taking the place of PPh$_3$ where possible (**II**, **III**, **VIII**−**XI**). Also similarly, the initial complexation of Pd(OAc)$_2$ to alkynylbenzamide **I** or alkyne **2a** is exergonic (−9.4 and −10.5 kcal/mol, respectively). However, comparison between the energy profiles with and without PPh$_3$ reveals some interesting differences. Thus, the combined results presented in Figures 3 and 4 would suggest again a competition between pathways A and B, but in this case pathway B would have an initial driving force advantage, since Pd(OAc)$_2$ tends to coordinate the terminal alkyne **2a** with higher affinity than for the alkynylbenzamide **I**. Cyclization is predicted to be the regiochemistry-determining step in both pathways, since the reverse reactions have much higher activation energies than the subsequent forward reactions. Interestingly, in pathway A, where the cyclization promoter is Pd(OAc)$_2$, the activation energy difference between the exo and endo cyclization modes is relatively small ($\Delta\Delta G^{\ddagger}$ = 0.3 kcal/mol, Figure 3) and, as a result, calculations predict a lower exo selectivity for pathway A in comparison with pathway B ($\Delta\Delta G^{\ddagger}$ = 1.7 kcal/mol). Therefore, according to calculations, the final exo/endo ratio in this reaction could be partially determined by the partition of Pd(OAc)$_2$ between an initial coordination to the benzamide alkynyl moiety (pathway A, low exo selectivity) and the alternative more favorable coordination to the terminal alkyne (pathway B, high exo selectivity). It is also noticed that, in the prevailing exo mode, pathway B has overall lower activation energies than pathway A, all of this suggesting that in the absence of phosphine pathway B could be a more competitive pathway in comparison to the case with PPh$_3$. Furthermore, the reactivity model depicted in Figures 3 and 4 may be representative of a more realistic situation where a weak donor ligand, such as DMF, occupies the vacant coordination position in the absence of PPh$_3$. In fact, this could happen even when PPh$_3$ is used, through exchange between DMF and PPh$_3$ or between DMF and the more labile phosphine oxide ligand[38] resulting from air oxidation of PPh$_3$ (see text above in connection with entries 15−17 of Table 1). Accordingly, in order to gain some insight into the energetics of those situations where Pd could be ligated to either a solvent molecule (DMF) or to a phosphine oxide, or have a vacant position, we have comparatively evaluated the energy balances of the competing complexation of **I** and **2a** to Pd(OAc)$_2$, either by themselves or in the presence of an additional ligand (PPh$_3$, OPPh$_3$, DMF). The corresponding results are displayed in Table 3, where trans complexes are used in all cases.

Table 3. Energetics of Equilibria (in kcal/mol)[a] between Alkyne Complexes of Pd(OAc)$_2$

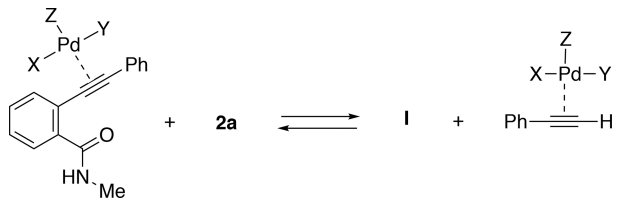

entry	X	Y	Z	ΔG°
1	OAc	OAc	*b*	−1.4
2	OAc	OAc	PPh$_3$	4.5
3	OAc	OAc	DMF	−8.5
4	OAc	OAc	OPPh$_3$	−1.0

[a] wB97XD/LANL2DZ/6-31G*//wB97XD-SMD (DMF)/LANL2DZ/6-31G*. [b] Agostic interaction with C−H from AcO Me group.

The data in Table 3 indicate a preference for coordination to the terminal alkyne in the presence of weak donor ligands (entries 1, 3, and 4),[47,38] while the comparatively stronger σ donor PPh$_3$, on the other hand, tends to stabilize the benzamide complex more than the terminal alkyne complex (entry 2). In line with previous literature reports, it is surmised that this effect could be due to an increased back-donation from a PPh$_3$-ligated Pd to the electron-deficient benzamide.[48] In any case, the driving force of the initial complexation step tends to favor either pathway A or B depending on the particular coordination at Pd, and pathway A would be favored at this stage only with PPh$_3$. It appears that pathway B could be an important contributor to the regioselectivity of the reaction in the other cases.

As mentioned above, heterocyclization appears to be the regiochemistry-determining step in these reactions. A comparison between the cyclization steps of pathways A and B provides an interesting opportunity to evaluate the effect of different Pd(II) species on the regiochemistry of cyclization. This situation arises because pathways A and B display distinct cyclization events where activation of the alkyne triple bond is provided either by a complex of type PdX$_2$ (mechanism A) or by an organometallic alkynylpalladium species RPdX (mechanism B). The calculation data presented in Figures 1−4 in all cases predict fast and exergonic cyclizations, with large differences between the forward and backward activation

DOI: 10.1021/acs.organomet.8b00519
Organometallics XXXX, XXX, XXX−XXX

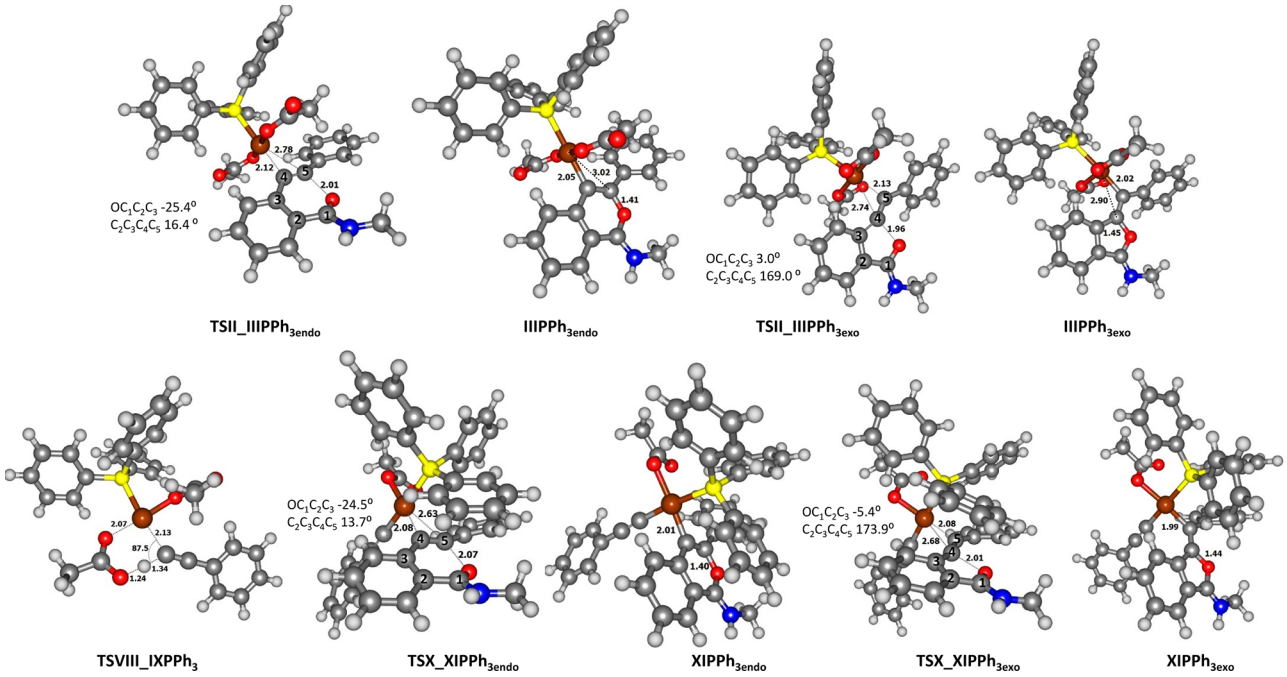

Figure 5. Selected structures from DFT calculations (red, oxygen; blue, nitrogen; brown, palladium; yellow, phosphorus; gray, carbon; white, hydrogen).[49]

Table 4. Calculated Effect of Ligands on the Exo/Endo Activation Energies (in kcal/mol)[a]

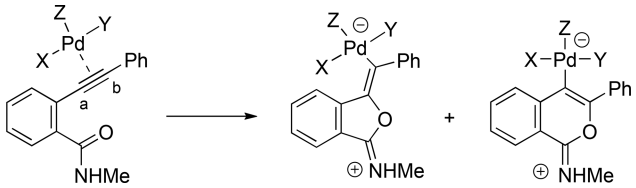

							exo		endo	
entry	X	Y	Z	$\Delta G^{\ddagger}_{exo}$	$\Delta G^{\ddagger}_{endo}$	$\Delta\Delta G^{\ddagger}_{exo,endo}$	Pd−C_a (Å)	C_a−O (Å)	Pd−C_b (Å)	C_b−O (Å)
1	Cl	Cl		2.4	0.5	1.9	2.44	2.24	2.52	2.22
2	Cl	Cl	PPh_3	6.3	7.2	−0.9	2.75	2.00	2.65	2.04
3	Cl		Cl	2.3	3.9	−1.6	2.64	2.09	2.63	2.09
4	Cl	PPh_3	Cl	2.7	4.6	−1.9	2.69	2.02	2.64	2.09
5[b]	Ph	PPh_3	Cl	1.5	7.7	−6.2	2.71	1.96	2.64	2.01
6	PhCC	PPh_3	Cl	3.0	6.1	−3.1	2.68	2.02	2.65	2.08
7	OAc	OAc	[c]	3.3	3.6	−0.3	2.57	2.18	2.62	2.17
8	OAc	OAc	PPh_3	4.6	9.6	−5.0	2.73	1.96	2.78	2.00

[a]wB97XD/LANL2DZ/6-31G*//wB97XD-SMD (DMF)/LANL2DZ/6-31G*. [b]Data taken from ref 28. [c]Agostic interaction with C−H from AcO Me group.

barriers. On the other hand, the effect of the σ-alkynyl ligand is not obvious from these data. In the absence of PPh_3 (Figures 3 and 4), the presence of a σ-carbon ligand at Pd results in increasing *exo*-selectivity; however, the opposite is found when PPh_3 is coordinated to Pd (Figures 1 and 2). While these results offer no clear trend, it has to be noted that the cis−trans configuration of complexes of type **II** and **X** is not the same. Thus, for example, **IIPPh$_3$** and **VIIIPPh$_3$** (Figures 1 and 2) are trans complexes but after C−H palladation of **VIIIPPh$_3$** and complexation of **I** the resulting cyclization precursor **XPPh$_3$** is a cis complex (see also Figure 5). In order to have a meaningful evaluation of the effect of a carbon σ ligand, we have studied the cyclizations of geometrically comparable complexes derived from $PdCl_2(PPh_3)_2$, a catalyst that has been experimentally found to also provide preferentially the exo product (Table 1, entry 10). These data are collected in Table 4, where we have also added for comparison the previously published cyclization energies on related arylation reactions,[28] as well as data taken from Figures 1 and 3 reflecting the effect of PPh_3 on the corresponding $Pd(OAc)_2$-promoted cyclizations.

The calculated results in Table 4 indicate that, when it is directly compared with a chloride ligand in the same position, a σ-carbon ligand increases the kinetic preference for an exo cyclization (entries 4−6). It is also observed that the presence of PPh_3 tends to favor kinetically the exo cyclization mode (entries 1−4, 7, and 8) and that the magnitude of this effect depends on the geometry of the palladium complex. For example, upon addition of a PPh_3 ligand to a trans $PdCl_2$ complex (entries 1 and 2) there is a 2.8 kcal/mol decrease in

DOI: 10.1021/acs.organomet.8b00519
Organometallics XXXX, XXX, XXX−XXX

$\Delta\Delta G^{\ddagger}_{exo,endo}$, favoring the exo cyclization, but the difference is only 0.3 kcal/mol with a cis geometry (entries 3 and 4). In line with entries 1 and 2, the low exo selectivity predicted for cyclizations promoted by a phosphine-free $Pd(AcO)_2$ turns into a very strong exo preference in the PPh_3-ligated complex (entries 7 and 8). It is suggested that, relative to the cases in entries 1 and 7, in the corresponding entries 2 and 8 the benzamide C−C triple bond is less activated toward cyclization because of the trans effect of the Z ligand PPh_3. This is reflected in higher activation energies and much less exergonic reactions in the latter cases, as exemplified by the energies of entries 7 and 8 displayed in Figures 1 and 3. At the same time, in the presence of the trans ligands the cyclization TSs show a more advanced formation of the C−O bond, as indicated by both the geometric characteristics of exo/endo TSs (Table 4; see also Figure 5) and NBO data showing the extent of the C−O interaction (see Table S4 and Figure S3 in the Supporting Information). As a result, in those cases the more planar exo TSs could benefit more from conjugation than the endo TSs, thus leading to higher exo selectivity. In line with these ideas, a comparison between entries 3 and 4 indicates that, once a trans ligand (Cl) is present, the addition of PPh_3 has little effect on the selectivity. Finally, it is apparent that the σ-carbon ligand reinforces the exo effect of the trans ligand (entries 4−6) but the reasons for this effect are not immediately obvious. In any case, from a practical point of view, this effect of the carbon ligand would be expected to be particularly relevant in those situations described above (Table 3) where pathway B is likely to be dominant.

■ SUMMARY AND CONCLUSIONS

Under oxidative Pd(II)-catalyzed conditions, 2-alkynylbenzamides and terminal alkynes participate in a cascade process that combines O-cyclization and a Sonogashira-type coupling. This leads to the formation of isobenzofuranimine derivatives as a result of a prevailing 5-exo cyclization mode. Insights into the mechanism of this reaction have been obtained with the aid of DFT calculations focused on two competing pathways that share participating cyclization, alkyne C−H palladation, and reductive elimination steps but differ in the order of cyclization and C−H palladation events. Precedent for a cyclization-first pathway is found in the related cyclization−alkynylation of *o*-alkynyldimethylanilines, which has been shown to take place with initial Pd(II)-promoted cyclization, followed by alkyne C−H palladation.[18,19] On the other hand, our results (experiments and DFT calculations) suggest that an alternative mechanism (C−H palladation first), where the order of cyclization and C−H palladation steps is reversed, could also be operative in the corresponding reactions of alkynylbenzamides. Thus, in a control test, treatment of an alkynylbenzamide with an isolated σ-alkynylpalladium(II), under otherwise standard reaction conditions, triggered formation of the corresponding alkynylated isobenzofuranimine product with exo selectivity, indicating that alkyne C−H palladation followed by cyclization is indeed a viable pathway in these reactions. According to calculations, this pathway is more likely to be followed in the absence of PPh_3 or in the presence of the weak ligand donors DMF and triphenylphosphine oxide. This stems from an initial partition of $Pd(OAc)_2$ between coordination to the benzamide alkynyl moiety (cyclization first pathway) or to the terminal alkyne (C−H palladation first pathway), where the latter is more favorable for those particular cases. In fact, since under the experimental conditions PPh_3 is observed to undergo oxidation to triphenylphosphine oxide, multiple realistic scenarios appear possible where different types of Pd(II) complexes (with phosphine, phosphine oxide, or solvent ligands) could catalyze the reaction. Finally, calculations also suggest that cyclization is the regiochemistry-determining step and that the presence on the palladium complex of a phosphine ligand and/or, significantly, *a C−Pd σ bond* (as in the C−H palladation first pathway) contributes significantly to the high exo selectivity observed in these reactions, each acting by a different mechanistic pathway.

■ EXPERIMENTAL SECTION

General Methods. Commercial DMF (≥99.8%) was kept over 4 Å MS. Routine NMR spectra were obtained at 25 °C on a Bruker AV-300 spectrometer (300 MHz for ^{1}H and 75 MHz for ^{13}C), a Bruker ARX-400 spectrometer (400 MHz for ^{1}H and 100 MHz for ^{13}C), and a Bruker AV-500 spectrometer (500 MHz for ^{1}H and 125 MHz for ^{13}C), using $CDCl_3$ and $(CD_3)_2CO$ as solvents and internal reference ($CDCl_3$ δ 7.26 for ^{1}H and δ 77.0 for ^{13}C, $[CD_3)_2CO$ δ 2.05 for ^{1}H and δ 29.84 for ^{13}C]. Chemical shifts (δ) are reported in ppm, and coupling constants (J) are given in hertz (Hz). The proton spectra are reported as follows: multiplicity, coupling constant J, number of protons, assignment. The DEPT sequence was routinely used for ^{13}C multiplicity assignment. Additionally, a combination of COSY, HSQC, HMBC, and NOESY NMR experiments was used for structural assignments. Infrared (IR) spectral data were obtained from a thin film deposited onto a NaCl glass and were measured on a Jasco FT/IR 4100 instrument in the interval between 4000 and 600 cm^{-1} with a 4 cm^{-1} resolution; data include only characteristic absorptions. Electrospray ionization (ESI$^+$) mass spectra were obtained on a micrOTOF focus mass spectrometer (Bruker Daltonics) using an ApolloII (ESI) source with a voltage of 4500 V applied to the capillary. Flash chromatography was carried out with silica gel (230−400 mesh) or using an automated Isco Combiflash Rf+ system with silica gel P60 (Silicycle). Analytical thin-layer chromatography (TLC) was performed on aluminum plates with Merck Kieselgel 60F254 and visualized by UV irradiation (254 nm). Preparative thin-layer chromatography was performed on silica gel plates (Si60+F254, 15 μm, 0.5 mm, 20 × 20 cm). Melting points were measured in a Büchi B-540 apparatus in open capillary tubes. New compounds were fully characterized by their ^{1}H and ^{13}C NMR, IR, and HRMS spectral properties. The structural assignments were confirmed by X-ray analysis of products **3k** and **4a** (Figures S1 and S2 in the Supporting Information).

General Procedures for Pd-Catalyzed Cyclization−Alkynylation. *Conditions A.* In a typical experiment, a terminal alkyne (0.468 mmol) was added to a solution of **1** (0.234 mmol), $Pd(OAc)_2$ (2.63 mg, 0.012 mmol), PPh_3 (6.10 mg, 0.023 mmol), and KI (19.0 mg, 0.120 mmol) in DMF (2 mL), and the mixture was stirred at 35 °C under air for the time indicated in Table 2. After the mixture was cooled to 25 °C, a saturated $NaHCO_3$ solution (5 mL) was added, and the mixture was extracted with EtOAc (3 × 10 mL). The combined organic layers were washed with water (5 mL) and dried (Na_2SO_4). The residue after evaporation was purified as indicated below for the individual cases to afford the products in the yields given in Table 2.

Conditions B. These reactions were carried out as in conditions A, with the addition of NaOAc (0.1 equiv). Additional preparation details and characterization data are as follows.

*(1Z,3E)-N-Butyl-3-(1,3-diphenylprop-2-yn-1-ylidene)-isobenzofuran-1(3H)-imine (**3a**) and (Z)-N-Butyl-3-phenyl-4-(phenylethynyl)-1H-isochromen-1-imine (**4a**).* Prepared from **1a**[50] and phenylacetylene (**2a**) using conditions A. The crude product was purified by flash chromatography (automated, solvent A 98/2 hexane/Et_3N; solvent B EtOAc; gradient from 100/0 to 90/10 A/B) to afford **4a**, **3a**, and **5a**.[32] Data for **3a**: brown solid, mp 61−62 °C. ^{1}H NMR [400 MHz, $(CD_3)_2CO$]: δ 8.68 (dt, J = 8.0, 0.9 Hz, 1H), 8.07−8.03

DOI: 10.1021/acs.organomet.8b00519
Organometallics XXXX, XXX, XXX−XXX

(m, 2H), 7.88 (dt, J = 7.6, 1.0 Hz, 1H), 7.75 (td, J = 7.6 Hz, 1H), 7.70−7.66 (m, 2H), 7.62 (td, J = 7.5, 1.0 Hz, 1H), 7.51−7.44 (m, 5H), 7.36 (tt, J = 7.5, 1.2 Hz, 1H), 3.66 (t, J = 7.0 Hz, 2H), 1.68 (quint, J = 7.3 Hz, 2H), 1.48 (sext, J = 7.3 Hz, 2H), 0.96 (t, J = 7.3 Hz, 3H). ^{13}C NMR [100 MHz, $(CD_3)_2CO$]: δ 153.4 (s), 153.0 (s), 137.0 (s), 136.3 (s), 132.9 (d), 132.2 (d, 2×), 131.4 (d), 131.3 (s), 129.8 (d, 2×), 129.7 (d, 2×), 129.7 (d), 129.1 (d, 2×), 128.6 (d), 124.8 (d), 123.9 (s), 123.7 (d), 100.5 (s), 97.2 (s), 88.3 (s), 48.6 (t), 33.7 (t), 21.3 (t), 14.2 (q). FTIR (NaCl): ν 2196 (w, C≡C), 1704 (s, C═N), 1590 (m, C═C) cm^{-1}. HRMS (ESI$^+$): calcd for $C_{27}H_{24}NO$ ([M + H]$^+$) 378.1852, found 378.1846. Data for **4a**: yellow solid, mp 115−116 °C (4/1 hexane/EtOAc). ^{1}H NMR [400 MHz, $(CD_3)_2CO$]: δ 8.27−8.20 (m, 3H), 7.99 (d, J = 7.6 Hz, 1H), 7.71 (td, J = 7.8, 1.3 Hz, 1H), 7.63−7.54 (m, 5H), 7.50 (td, J = 7.7, 1.2 Hz, 1H), 7.46−7.41 (m, 3H), 3.62 (t, J = 7.0 Hz, 2H), 1.69 (quint, J = 7.1 Hz, 2H), 1.52 (sext, J = 7.2 Hz, 2H), 0.97 (t, J = 7.3 Hz, 3H). ^{13}C NMR [100 MHz, $(CD_3)_2CO$]: δ 156.7 (s), 148.1 (s), 134.3 (s), 132.9 (d), 132.0 (d, 2×), 131.1 (d, 2×), 129.6 (s), 129.6 (d), 129.5 (d), 129.4 (d), 129.2 (d, 2×), 129.1 (d, 2×), 127.2 (d), 125.6 (d), 124.3 (s), 124.0 (s), 98.5 (s), 97.3 (s), 84.5 (s), 46.6 (t), 33.8 (t), 21.4 (t), 14.3 (q). FTIR (NaCl): ν 1666 (s, C═N), 1603 (m, C═C) cm^{-1}. HRMS (ESI$^+$): calcd for $C_{27}H_{24}NO$ ([M + H$^+$]) 378.1852, found 378.1847.

*(1Z,3E)-N-Butyl-3-[3-(cyclohex-1-en-1-yl)-1-(4-methoxyphenyl)-prop-2-yn-1-ylidene]isobenzofuran-1(3H)-imine (**3b**).* Prepared from **1b**[33] and 1-ethynylcyclohexene (**2b**) using conditions B. The crude product was purified by flash chromatography (automated, solvent A 98/2 hexane/Et_3N; solvent B EtOAc; gradient from 100/0 to 85/15 A/B) to afford **3b** as a yellow oil. ^{1}H NMR [400 MHz, $(CD_3)_2CO$]: δ 8.60 (dt, J = 8.0, 0.9 Hz, 1H), 7.98−7.93 (m, 2H), 7.87 (dt, J = 7.6, 1.0 Hz, 1H), 7.73 (td, J = 7.6, 1.1 Hz, 1H), 7.61 (td, J = 7.5, 0.9 Hz, 1H), 7.06−7.00 (m, 2H), 6.35 (tt, J = 4.0, 1.9 Hz, 1H), 3.86 (s, 3H), 3.67 (t, J = 6.9 Hz, 2H), 2.40−2.33 (m, 2H), 2.25−2.18 (m, 2H), 1.79−1.63 (m, 6H), 1.48 (sext, J = 7.4 Hz, 2H), 0.96 (t, J = 7.5 Hz, 3H). ^{13}C NMR [100 MHz, $(CD_3)_2CO$]: δ 160.2 (s), 153.7 (s), 151.1 (s), 137.2 (s), 136.2 (d), 132.7 (d), 131.1 (d, 2×), 131.0 (s), 130.8 (d), 128.7 (s), 124.5 (d), 123.6 (d), 121.8 (s), 114.4 (d, 2×), 100.9 (s), 99.4 (s), 85.9 (s), 55.6 (q), 48.5 (t), 33.7 (t), 29.7 (t), 26.4 (t), 23.0 (t), 22.2 (t), 21.3 (t), 14.2 (q). FTIR (NaCl): ν 1699 (s, C═N), 1605 (m, C═C) cm^{-1}. HRMS (ESI$^+$): calcd for $C_{28}H_{30}NO_2$ ([M + H]$^+$) 412.2271, found 412.2272.

*Methyl 4-{1-[(1E,3Z)-3-(Butylimino)isobenzofuran-1(3H)-ylidene]-3-(4-methoxyphenyl)prop-2-yn-1-yl}benzoate (**3c**).* Prepared from **1c**[33] and 4-ethynylanisole (**2c**) using conditions A. The crude product was purified by flash chromatography (automated, solvent A 98/2 hexane/Et_3N; solvent B EtOAc; gradient from 100/0 to 85/15 A/B) to afford **3c** as a yellow solid, mp 103−104 °C. ^{1}H NMR (400 MHz, $CDCl_3$): δ 8.60 (d, J = 7.8 Hz, 1H), 8.13−8.04 (m, 4H), 7.92 (d, J = 7.6 Hz, 1H), 7.60 (dt, J = 7.6, 1.0 Hz, 1H), 7.55−7.50 (m, 3H), 6.97−6.91 (m, 2H), 3.94 (s, 3H), 3.85 (s, 3H), 3.68 (t, J = 7.1 Hz, 2H), 1.72 (quint, J = 7.3 Hz, 2H), 1.47 (sext, J = 7.4 Hz, 2H), 0.98 (t, J = 7.4 Hz, 3H). ^{13}C NMR (100 MHz, $CDCl_3$): δ 167.0 (s), 160.1 (s), 153.6 (s), 152.8 (s), 140.4 (s), 136.3 (s), 133.1 (d, 2×), 131.9 (d), 130.5 (d), 130.4 (s), 129.5 (d, 2×), 129.0 (d, 2×), 128.8 (s), 124.3 (d), 123.1 (d), 115.2 (s), 114.4 (d, 2×), 99.6 (s), 97.0 (s), 85.8 (s), 55.5 (q), 52.3 (q), 48.5 (t), 33.0 (t), 20.9 (t), 14.1 (q). FTIR (NaCl): ν 2196 (w, C≡C), 1718 (s, C═N, C═O) cm^{-1}. HRMS (ESI$^+$): calcd for $C_{30}H_{28}NO_4$ ([M + H]$^+$) 466.2013, found 466.2001.

*Methyl 4-(1-((1E,3Z)-3-(Butylimino)isobenzofuran-1(3H)-ylidene)-3-(cyclohex-1-en-1-yl)prop-2-yn-1-yl)benzoate (**3d**) and [N(Z),N′(Z)]-N,N′-{[1,2-Bis(4-carbomethoxyphenyl)-1,2-ethanediylidene]bis[(3E)-3,1-isobenzofurandiylidene]}-bisbutylamine (**5d**).* Prepared from **1c**[33] and 1-ethynylcyclohexene (**2b**) using conditions A. The crude product was purified by flash chromatography (automated, solvent A 98/2 hexane/Et_3N; solvent B EtOAc; gradient from 100/0 to 85/15 A/B) to afford **3d** and **5d** as brown solids. Data for **3d**: mp 82−83 °C. ^{1}H NMR (400 MHz, $CDCl_3$): δ 8.54 (dt, J = 8.0, 0.9 Hz, 1H), 8.09−8.04 (m, 2H), 8.04−7.99 (m, 2H), 7.90 (dt, J = 7.7, 0.9 Hz, 1H), 7.60 (td, J = 7.5, 1.0 Hz, 1H), 7.51 (td, J = 7.5, 1.0 Hz, 1H), 6.33−6.29 (m, 1H), 3.93 (s, 3H), 3.66 (t, J = 7.1 Hz, 2H), 2.35−2.30 (m, 2H), 2.24−2.18 (m, 2H), 1.78−1.63 (m, 6H), 1.45 (sext, J = 7.6 Hz, 2H), 0.96 (t, J = 7.4 Hz, 3H). ^{13}C NMR (100 MHz, $CDCl_3$): δ 167.0 (s), 153.6 (s), 152.5 (s), 140.5 (s), 136.4 (s), 136.0 (d), 131.8 (d), 130.4 (d), 130.3 (s), 129.4 (d, 2×), 128.9 (d, 2×), 128.7 (s), 124.3 (d), 123.1 (d), 120.9 (s), 99.8 (s), 99.1 (s), 84.6 (s), 52.2 (q), 48.5 (t), 33.0 (t), 29.1 (t), 26.0 (t), 22.4 (t), 21.6 (t), 20.9 (t), 14.1 (q). FTIR (NaCl): ν 2181 (w, C≡C), 1718 (s, C═N, C═O), 1599 (m, C═C) cm^{-1}. HRMS (ESI$^+$): calcd for $C_{29}H_{30}NO_3$ ([M + H]$^+$) 440.2220, found 440.2217. Data for **5d**: mp 81−82 °C (4/1 hexane/EtOAc). ^{1}H NMR (400 MHz, $CDCl_3$): δ 8.02−7.98 (m, 4H), 7.96−7.92 (m, 4H), 7.84 (dt, J = 7.7, 1.0 Hz, 2H), 7.49 (dt, J = 8.0, 0.9 Hz, 2H), 7.36 (td, J = 7.5, 1.0 Hz, 2H), 7.26 (td, J = 7.6, 1.0 Hz, 2H), 3.88 (s, 6H), 3.84−3.76 (m, 4H), 1.84−1.75 (m, 4H), 1.56 (sext, J = 7.6 Hz, 4H), 1.03 (t, J = 7.3 Hz, 6H). ^{13}C NMR (100 MHz, $CDCl_3$): δ 166.8 (s, 2×), 154.0 (s, 2×), 150.3 (s, 2×), 140.5 (s, 2×), 136.0 (s, 2×), 132.3 (d, 2×), 130.8 (s, 2×), 130.5 (d, 2×), 130.0 (d, 4×), 129.1 (d, 4×), 129.2 (s, 2×), 123.6 (d, 2×), 123.3 (d, 2×), 111.8 (s, 2×), 52.3 (q, 2×), 48.5 (t, 2×), 32.1 (t, 2×), 20.9 (t, 2×), 14.2 (q, 2×). FTIR (NaCl): ν 1715 (s, C═N, C═O), 1604 (m, C═C) cm^{-1}. HRMS (ESI$^+$): calcd for $C_{42}H_{41}N_2O_6$ ([M + H]$^+$) 669.2959, found 669.2940.

*Methyl 4-{1-[(1E,3Z)-3-(Butylimino)isobenzofuran-1(3H)-ylidene]-3-phenylprop-2-yn-1-yl}benzoate (**3e**).* Prepared from **1c**[33] and phenylacetylene (**2a**) using conditions B. The crude product was purified by flash chromatography (automated, solvent A 98/2 hexane/Et_3N; solvent B EtOAc; gradient from 100/0 to 85/15 A/B) to afford **3e** as a yellow solid, mp 119−120 °C. ^{1}H NMR [400 MHz, $(CD_3)_2CO$]: δ 8.72 (d, J = 7.6 Hz, 1H), 8.23−8.17 (m, 2H), 8.15−8.09 (m, 2H), 7.92 (d, J = 7.5 Hz, 1H), 7.81 (t, J = 7.6, 1H), 7.75−7.66 (m, 3H), 7.53−7.47 (m, 3H), 3.92 (s, 3H), 3.71 (t, J = 7.0 Hz, 2H), 1.70 (quint, J = 7.1 Hz, 2H), 1.48 (sext, J = 7.3 Hz, 2H), 0.96 (t, J = 7.4 Hz, 3H). ^{13}C NMR [100 MHz, $(CD_3)_2CO$]: δ 166.9 (s), 154.2 (s), 153.0 (s), 141.0 (s), 136.8 (s), 133.2 (d), 132.3 (d, 2×), 132.0 (d), 131.5 (s), 130.2 (d, 2×), 129.9 (d), 129.8 (d, 2×), 129.7 (d, 2×), 125.1 (d), 123.9 (d), 123.9 (s), 123.7 (s), 99.5 (s), 97.6 (s), 87.6 (s), 52.4 (c) 48.8 (t), 33.7 (t), 21.3 (t), 14.2 (c). FTIR (NaCl): ν 1715 (s, C═N, C═O), 1587 (m, C═C) cm^{-1}. HRMS (ESI$^+$): calcd for $C_{29}H_{26}NO_3$ (M+1) 436.1907, found 436.1897.

*(1Z,3E)-3-[1,3-Bis(4-Methoxyphenyl)prop-2-yn-1-ylidene]-N-phenylisobenzofuran-1(3H)-imine (**3f**).* Prepared from **1d**[32] and 4-ethynylanisole (**2c**) using conditions A. The crude product was purified by flash chromatography (automated, solvent A 98/2 hexane/Et_3N; solvent B EtOAc; gradient from 100/0 to 85/15 A/B) to afford **3f** as a yellow solid, mp 168−169 °C. ^{1}H NMR (400 MHz, $CDCl_3$): δ 8.60 (d, J = 7.9 Hz, 1H), 8.06 (d, J = 7.6 Hz, 1H), 7.96−7.90 (m, 2H), 7.65 (td, J = 7.6, 1.1 Hz, 1H), 7.59−7.51 (m, 3H), 7.50−7.44 (m, 2H), 7.42−7.35 (m, 2H), 7.19 (tt, J = 7.3, 1.2 Hz, 1H), 6.98−6.92 (m, 2H), 6.91−6.84 (m, 2H), 3.86 (s, 3H), 3.85 (s, 3H). ^{13}C NMR (100 MHz, $CDCl_3$): δ 160.1 (s), 159.4 (s), 153.2 (s), 150.6 (s), 145.7 (s), 136.5 (s), 133.1 (d, 2×), 132.5 (d), 130.6 (d, 2×), 130.3 (s), 129.9 (d), 128.8 (d, 2×), 127.7 (s), 125.1 (d), 124.1 (d, 2×), 123.9 (d), 123.7 (d), 115.3 (s), 114.4 (d, 2×), 113.6 (d, 2×), 102.0 (s), 97.2 (s), 86.3 (s), 55.5 (q), 55.4 (q). FTIR (NaCl): ν 2196 (w, C≡C), 1681 (s, C═N), 1602 (m, C═C) cm^{-1}. HRMS (ESI$^+$): calcd for $C_{31}H_{24}NO_3$ ([M + H]$^+$) 458.1751, found 458.1742.

*(1Z,3E)-3-[1-(4-Methoxyphenyl)-3-(thiophen-3-yl)prop-2-yn-1-ylidene]-N-phenylisobenzofuran-1(3H)-imine (**3g**).* Prepared from **1d**[32] and 3-ethynylthiophene (**2d**) using conditions A. The crude product was purified by flash chromatography (automated, solvent A 98/2 hexane/Et_3N; solvent B EtOAc; gradient from 100/0 to 85/15 A/B) to afford **3g** as a brown solid, mp 144−145 °C. ^{1}H NMR (400 MHz, $CDCl_3$): δ 8.57 (dt, J = 7.9, 0.9 Hz, 1H), 8.06 (dt, J = 7.6, 1.1 Hz, 1H), 7.93−7.88 (m, 2H), 7.69−7.60 (m, 2H), 7.56 (td, J = 7.5, 1.0 Hz, 1H), 7.48−7.43 (m, 2H), 7.42−7.36 (m, 3H), 7.29 (dd, J = 5.0, 1.2 Hz, 1H), 7.22−7.17 (m, 1H), 6.91−6.86 (m, 2H), 3.85 (s, 3H). ^{13}C NMR (100 MHz, $CDCl_3$): δ 159.5 (s), 153.0 (s), 151.0 (s), 145.6 (s), 136.4 (s), 132.5 (d), 130.6 (d, 2×), 130.3 (s), 130.1 (d), 129.8 (d), 129.1 (d), 128.8 (d, 2×), 127.5 (s), 126.0 (d), 125.2 (d), 124.1 (d, 2×), 123.8 (d), 123.7 (d), 122.3 (s), 113.7 (d, 2×), 101.6 (s), 92.3 (s), 87.1 (s), 55.5 (q). FTIR (NaCl): ν 2201 (w, C≡C),

DOI: 10.1021/acs.organomet.8b00519
Organometallics XXXX, XXX, XXX−XXX

1681 (s, C═N), 1593 (m, C═C) cm^{-1}. HRMS (ESI^+): calcd for $C_{28}H_{20}NO_2S$ ([M + H]$^+$) 434.1209, found 434.1202.

*(1Z,3E)-3-(1,3-Diphenylprop-2-yn-1-ylidene)-N-phenylisobenzofuran-1(3H)-imine (**3h**).*[37b] Prepared from **1e**[51] and phenylacetylene (**2a**) using conditions A. The crude product was purified by flash chromatography (silica gel saturated with Et_3N, 95/3/2 hexanes/EtOAc/Et_3N) to afford **3h**[37b] as an oil.

*(1Z,3E)-N-Butyl-3-(1-phenylnon-1-yn-3-ylidene)isobenzofuran-1(3H)-imine (**3i**).* Prepared from **1f**[52] and phenylacetylene (**2a**) using conditions B. The crude product was purified by flash chromatography (automated, solvent A 98/2 hexane/Et_3N; solvent B EtOAc; gradient from 100/0 to 90/10 A/B) to afford **3i** as a brown solid, mp 62−63 °C. ^{1}H NMR [400 MHz, $(CD_3)_2CO$]: δ 8.50 (dt, J = 7.9, 0.9 Hz, 1H), 7.96 (dt, J = 7.7, 1.0 Hz, 1H), 7.75 (td, J = 7.6, 1.1 Hz, 1H), 7.65−7.60 (m, 3H), 7.57−7.52 (m, 2H), 7.49−7.42 (m, 3H), 6.99−6.95 (m, 2H), 3.83 (s, 3H), 2.64 (t, J = 7.5 Hz, 2H), 1.76 (quint, J = 7.5 Hz, 2H), 1.50−1.42 (m, 2H), 1.41−1.29 (m, 4H), 0.88 (t, J = 7.1 Hz, 3H). ^{13}C NMR [100 MHz, $(CD_3)_2CO$]: δ 158.4 (s), 153.4 (s), 151.4 (s), 139.0 (s), 135.6 (s), 133.2 (d), 132.3 (s), 132.1 (d, 2×), 131.0 (d), 129.6 (d, 2×), 129.5 (d), 127.2 (d, 2×), 124.1 (s), 124.0 (d), 123.8 (d), 114.8 (d, 2×), 102.7 (s), 97.8 (s), 88.4 (s), 57.7 (q), 32.3 (t), 31.8 (t), 29.5 (t), 28.8 (t), 23.3 (t), 14.4 (q). FTIR (NaCl): ν 2190 (w, C≡C), 1681 (s, C═N), 1502 (s, C═C) cm^{-1}. HRMS (ESI^+): calcd for $C_{30}H_{30}NO_2$ ([M + H]$^+$) 436.2271, found 436.2265.

*(1Z,3E)-N-Butyl-3-(1-phenylnon-2-yn-1-ylidene)isobenzofuran-1(3H)-imine (**3j**).* Prepared from **1a**[50] and 1-octyne (**2e**) using conditions A. The crude product was purified by flash chromatography (97/2/1 hexanes/EtOAc/Et_3N) to afford **3j** as an oil. ^{1}H NMR [300 MHz, $(CD_3)_2CO$]: δ 8.61 (dt, J = 7.9, 0.9 Hz, 1H), 8.04−7.95 (m, 2H), 7.85 (dt, J = 7.5, 1.0 Hz, 1H), 7.68 (td, J = 7.6, 1.3 Hz, 1H), 7.60 (td, J = 7.5, 1.1 Hz, 1H), 7.48−7.39 (m, 2H), 7.35−7.28 (m, 1H), 3.63 (t, J = 6.9 Hz, 2H), 2.65 (t, J = 7.0 Hz, 2H), 1.79−1.30 (m, 12H), 0.98−0.86 (m, 6H). ^{13}C NMR [75 MHz, $(CD_3)_2CO$]: δ 153.6 (s), 152.2 (s), 137.2 (s), 136.9 (s), 132.6 (d), 131.1 (d), 129.8 (d), 128.9 (d), 128.4 (d), 124.6 (d), 123.6 (d), 101.2 (s), 99.1 (s), 79.1 (s), 48.5 (t), 33.7 (t), 32.1 (t), 29.5 (t), 29.4 (t), 23.3 (t), 21.3 (t), 20.3 (t), 14.3 (q), 14.2 (q). IR (NaCl): ν 1703 (s, C═N) cm^{-1}. HRMS (ESI^+): calcd for $C_{27}H_{32}NO$ [M + H]$^+$ 386.2484, found 386.2483.

*(1Z,3E)-N-Benzyl-3-(1,3-diphenylprop-2-yn-1-ylidene)-isobenzofuran-1(3H)-imine (**3k**).* Prepared from **1g**[37b] and phenylacetylene (**2a**) using conditions A. The crude product was purified by preparative TLC (silica gel saturated with Et_3N, 90/8/2 hexanes/EtOAc/Et_3N) to afford **3k**. The X-ray sample was crystallized from 4/1 acetone/water. ^{1}H NMR [300 MHz, $(CD_3)_2CO$]: δ 8.71 (dt, J = 8.0, 1.0 Hz, 1H), 8.09−7.99 (m, 2H), 7.96 (dt, J = 7.7, 1.1 Hz, 1H), 7.81 (td, J = 7.7, 1.3 Hz, 1H), 7.74−7.63 (m, 3H), 7.55−7.30 (m, 10H), 7.28−7.19 (m, 1H), 4.89 (s, 2H). ^{13}C NMR [75 MHz, $(CD_3)_2CO$]: δ 154.3 (s), 152.9 (s), 141.2 (s), 137.0 (s), 136.2 (s), 133.2 (d), 132.2 (d), 131.5 (d), 131.2 (s), 129.9 (d), 129.7 (d), 129.7 (d), 129.2 (d), 129.1 (d), 128.8 (d), 128.6 (d), 127.5 (d), 124.8 (d), 123.9 (d), 123.8 (s), 101.1 (s), 97.4 (s), 88.2 (s), 52.5 (t). IR (NaCl): ν 1698 (s, C═N) cm^{-1}. HRMS (ESI^+): calcd for $C_{30}H_{22}NO$ [M + H]$^+$ 412.1701, found 412.1709.

*(1Z,3E)-N-(4-Chlorophenyl)-3-(1-phenylnon-1-yn-3-ylidene)-isobenzofuran-1(3H)-imine (**3l**).* Prepared from **1h**[32] and phenylacetylene (**2a**) using conditions A. The crude product was purified by preparative TLC (silica gel saturated with Et_3N, 96/2/2 hexanes/EtOAc/Et_3N) to afford **3l** as an oil. ^{1}H NMR [300 MHz, $(CD_3)_2CO$]: δ 8.49 (dt, J = 7.9 Hz, 0.9 Hz, 1H), 7.97 (dt, J = 7.7, 0.9 Hz, 1H), 7.79 (td, J = 7.6, 1.1 Hz, 1H), 7.69−7.57 (m, 3H), 7.48−7.38 (m, 7H), 2.57 (t, J = 7.5 Hz, 2H), 1.77−1.68 (m, 2H), 1.47−1.25 (m, 6H), 0.84−0.88 (m, 3H). ^{13}C NMR [75 MHz, $(CD_3)_2CO$]: δ 153.6 (s), 153.1 (s), 145.3 (s), 136.0 (s), 133.8 (d), 132.2 (d), 131.6 (s), 131.1 (d), 130.4 (s), 129.6 (d, 2×), 126.7 (d), 124.3 (d), 123.9 (s), 123.8 (d), 103.8 (s), 98.2 (s), 88.1 (s), 32.3 (t), 31.7 (t), 29.5 (t), 28.8 (t), 23.3 (t), 14.4 (q). IR (NaCl): ν 1682 (s, C═N) cm^{-1}. HRMS (ESI^+): calcd for $C_{29}H_{27}NOCl$ [M + H]$^+$ 440.1781, found 440.1782.

Computational Methods. DFT calculations with the hybrid functionals ωB97XD (with dispersion correction)[53] have been carried out using Gaussian09[54] to characterize the stationary points on the potential energy surface at the 6-31G*[53a] level for all atoms with the exception of palladium, for which the LANL2DZ effective core potential[55] and the corresponding basis set were used. The optimized geometries have been characterized by harmonic analysis, and the nature of the stationary points was determined according to the number of negative eigenvalues of the Hessian matrix. Zero-point vibration energies (ZPVE) and thermal corrections (at 298 K, 1 atm) to the energy have been estimated using the computed frequencies with application of the free particle, harmonic oscillator, and rigid rotor approximations at the high-temperature limit in a canonical ensemble. The natural bond orbital analysis was made with the NBO program[56] implemented in Gaussian09. Solvation effects (DMF) have been also included as single-point corrections to the gas-phase free energy of the optimized structures computed with the ωB97XD functional with the self-consistent reaction field (SCRF) method using the SMD model as implemented in Gaussian09.[57]

■ ASSOCIATED CONTENT

Supporting Information

The Supporting Information is available free of charge on the ACS Publications website at DOI: 10.1021/acs.organomet.8b00519.

Additional experimental details, crystallographic data, energies of calculated structures, NBO data, and NMR spectra (PDF)

Cartesian coordinates for all computed structures (XYZ)

Accession Codes

CCDC 1555989 and 1560911 contain the supplementary crystallographic data for this paper. These data can be obtained free of charge via www.ccdc.cam.ac.uk/data_request/cif, or by emailing data_request@ccdc.cam.ac.uk, or by contacting The Cambridge Crystallographic Data Centre, 12 Union Road, Cambridge CB2 1EZ, UK; fax: +44 1223 336033.

■ AUTHOR INFORMATION

Corresponding Authors

*E-mail for R.A.: rar@uvigo.es.

*E-mail for J.M.A.: jm.aurrecoechea@ehu.eus.

ORCID

Rosana Álvarez: 0000-0001-5608-7561

José M. Aurrecoechea: 0000-0002-1523-4593

Notes

The authors declare no competing financial interest.

■ ACKNOWLEDGMENTS

The authors thank the Spanish Ministerio de Economía y Competitividad (MINECO) (grant numbers CTQ2012-37734 and CTQ2015-68794-P), Fondos Europeos para el Desarrollo Regional (FEDER), and the Universidad del País Vasco UPV/EHU (PES12/32 and fellowship to Y M. "*Ayuda para la Contratación de Doctores Recientes*") for financial support. SGIker UPV/EHU is thanked for technical support (NMR facilities, HRMS and X-ray analyses). We are grateful to the Centro de Supercomputación de Galicia (CESGA) for generous allocation of computing resources.

■ REFERENCES

(1) *Modern Alkyne Chemistry: Catalytic and Atom-Economic Transformations*; Trost, B. M., Li, C.-J., Eds.; Wiley-VCH: Weinheim, Germany, 2014.

DOI: 10.1021/acs.organomet.8b00519
Organometallics XXXX, XXX, XXX−XXX

(2) *Metal-Catalyzed Cross-Coupling Reactions and More*; de Meijere, A., Stefan Brase, S., Oestreich, M., Eds.; Wiley-VCH: Weinheim, Germany, 2014.
(3) Villarino, L.; García-Fandiño, R.; López, F.; Mascareñas, J. L. Palladium-Catalyzed Conjugate Addition of Terminal Alkynes to Enones. *Org. Lett.* **2012**, *14*, 2996−2999.
(4) Sanz-Marco, A.; Blay, G.; Munoz, M. C.; Pedro, J. R. Highly enantioselective copper(I)-catalyzed conjugate addition of 1,3-diynes to alpha,beta-unsaturated trifluoromethyl ketones. *Chem. Commun.* **2015**, *51*, 8958−8961.
(5) Li, Y. X.; Liu, L.; Kong, D. L.; Wang, D.; Feng, W. C.; Yue, T.; Li, C. J. Palladium-Catalyzed Alkynylation of Morita-Baylis-Hillman Carbonates with (Triisopropylsilyl)acetylene on Water. *J. Org. Chem.* **2015**, *80*, 6283−6290.
(6) Wang, H. N.; Hearne, Z.; Knauber, T.; Dalko, M.; Hitce, J.; Marat, X.; Moreau, M.; Li, C. J. Palladium-catalyzed 1,4-addition of terminal alkynes to acrolein. *Tetrahedron* **2015**, *71*, 5866−5870.
(7) HariBabu, M.; Dwivedi, V.; Kant, R.; Reddy, M. S. Palladium-Catalyzed Regio- and Stereoselective Cross-Addition of Terminal Alkynes to Ynol Ethers and Synthesis of 1,4-Enyn-3-ones. *Angew. Chem., Int. Ed.* **2015**, *54*, 3783−3786.
(8) Wang, W.; Shen, Y.; Meng, X.; Zhao, M.; Chen, Y.; Chen, B. Copper-Catalyzed Synthesis of Quinoxalines with o-Phenylenediamine and Terminal Alkyne in the Presence of Bases. *Org. Lett.* **2011**, *13*, 4514−4517.
(9) Shibahara, F.; Dohke, Y.; Murai, T. Palladium-Catalyzed C-H Bond Direct Alkynylation of 5-Membered Heteroarenes: A Well-Defined Synthetic Route to Azole Derivatives Containing Two Different Alkynyl Groups. *J. Org. Chem.* **2012**, *77*, 5381−5388.
(10) Kim, S. H.; Park, S. H.; Chang, S. Palladium-catalyzed oxidative alkynylation of arene C-H bond using the chelation-assisted strategy. *Tetrahedron* **2012**, *68*, 5162−5166.
(11) Jie, X. M.; Shang, Y. P.; Hu, P.; Su, W. P. Palladium-Catalyzed Oxidative Cross-Coupling between Heterocycles and Terminal Alkynes with Low Catalyst Loading. *Angew. Chem., Int. Ed.* **2013**, *52*, 3630−3633.
(12) Dong, J. X.; Wang, F.; You, J. S. Copper-Mediated Tandem Oxidative C(sp(2))-H/C(sp)-H Alkynylation and Annulation of Arenes with Terminal Alkynes. *Org. Lett.* **2014**, *16*, 2884−2887.
(13) Parsharamulu, T.; Reddy, P. V.; Likhar, P. R.; Kantarn, M. L. Dehydrogenative and decarboxylative C-H alkynylation of heteroarenes catalyzed by Pd(II)-carbene complex. *Tetrahedron* **2015**, *71*, 1975−1981.
(14) Ha, H.; Shin, C.; Bae, S.; Joo, J. M. Divergent Palladium-Catalyzed Cross-Coupling of Nitropyrazoles with Terminal Alkynes. *Eur. J. Org. Chem.* **2018**, *2018*, 2645−2650.
(15) Liu, L.; Zhou, D.; Liu, M.; Zhou, Y. B.; Chen, T. Q. Palladium-Catalyzed Decarbonylative Alkynylation of Amides. *Org. Lett.* **2018**, *20*, 2741−2744.
(16) Recent reviews: (a) Gabriele, B.; Mancuso, R.; Salerno, G. Oxidative Carbonylation as a Powerful Tool for the Direct Synthesis of Carbonylated Heterocycles. *Eur. J. Org. Chem.* **2012**, *2012*, 6825−6839. (b) Schultz, D. M.; Wolfe, J. P. Recent Developments in Palladium-Catalyzed Alkene Aminoarylation Reactions for the Synthesis of Nitrogen Heterocycles. *Synthesis* **2012**, *44*, 351−361. (c) Wu, X. F.; Neumann, H.; Beller, M. Synthesis of Heterocycles via Palladium-Catalyzed Carbonylations. *Chem. Rev.* **2013**, *113*, 1−35. (d) Gulevich, A. V.; Dudnik, A. S.; Chernyak, N.; Gevorgyan, V. Transition Metal-Mediated Synthesis of Monocyclic Aromatic Heterocycles. *Chem. Rev.* **2013**, *113*, 3084−3213. (e) Ye, J. T.; Ma, S. M. Palladium-Catalyzed Cyclization Reactions of Allenes in the Presence of Unsaturated Carbon-Carbon Bonds. *Acc. Chem. Res.* **2014**, *47*, 989−1000. (f) Le Bras, J.; Muzart, J. Palladium-catalysed inter- and intramolecular formation of C-O bonds from allenes. *Chem. Soc. Rev.* **2014**, *43*, 3003−3040. (g) Garlets, Z. J.; White, D. R.; Wolfe, J. P. Recent Developments in Pd-0-Catalyzed Alkene-Carboheterofunctionalization Reactions. *Asian J. Org. Chem.* **2017**, *6*, 636−653. (h) Chemler, S. R.; Karyakarte, S. D.; Khoder, Z. M. Stereoselective and Regioselective Synthesis of Heterocycles via Copper-Catalyzed Additions of Amine Derivatives and Alcohols to Alkenes. *J. Org. Chem.* **2017**, *82*, 11311−11325. (i) Broggini, G.; Borelli, T.; Giofre, S.; Mazza, A. Intramolecular Oxidative Palladium-Catalyzed Amination Involving Double C-H Functionalization of Unactivated Olefins. *Synthesis* **2017**, *49*, 2803−2818. (j) Li, J. X.; Yang, S. R.; Wu, W. Q.; Jiang, H. F. Recent Advances in Pd-Catalyzed Cross-Coupling Reaction in Ionic Liquids. *Eur. J. Org. Chem.* **2018**, *2018*, 1284−1306.
(17) Alcaide, B.; Almendros, P.; Rodriguez-Acebes, R. Pd-Cu bimetallic catalyzed domino cyclization of alpha-allenols followed by a coupling reaction: New sequence leading to functionalized spirolactams. *Chem. - Eur. J.* **2005**, *11*, 5708−5712.
(18) Yao, B.; Wang, Q.; Zhu, J. Palladium-Catalyzed Coupling of ortho-Alkynylanilines with Terminal Alkynes Under Aerobic Conditions: Efficient Synthesis of 2,3-Disubstituted 3-Alkynylindoles. *Angew. Chem., Int. Ed.* **2012**, *51*, 12311−12315.
(19) Yao, B.; Wang, Q.; Zhu, J. Mechanistic Study on the Palladium(II)-Catalyzed Synthesis of 2,3-Disubstituted Indoles Under Aerobic Conditions: Anion Effects and the Development of a Low-Catalyst-Loading Process. *Chem. - Eur. J.* **2014**, *20*, 12255−12261.
(20) Volla, C. M. R.; Backvall, J. E. Palladium-Catalyzed Oxidative Domino Carbocyclization- Carbonylation-Alkynylation of Enallenes. *Org. Lett.* **2014**, *16*, 4174−4177.
(21) Xia, Y.; Liu, Z.; Ge, R.; Xiao, Q.; Zhang, Y.; Wang, J. Pd-catalyzed cross-coupling of terminal alkynes with ene-yne-ketones: access to conjugated enynes via metal carbene migratory insertion. *Chem. Commun.* **2015**, *51*, 11233−11235.
(22) Yao, B.; Wang, Q.; Zhu, J. P. Pd/C-Catalyzed Cyclizative Cross-Coupling of Two ortho-Alkynylanilines under Aerobic Conditions: Synthesis of 2,3 ′-Bisindoles. *Chem. - Eur. J.* **2015**, *21*, 7413−7416.
(23) Ha, T. M.; Yao, B.; Wang, Q.; Zhu, J. P. 2-(Methoxycarbonyl)-ethyl as a Removable N-Protecting Group: Synthesis of Indoloisoquinolinones by Pd(II)-Catalyzed Intramolecular Diamination of Alkynes. *Org. Lett.* **2015**, *17*, 1750−1753.
(24) Thirupathi, N.; Puri, S.; Reddy, T. J.; Sridhar, B.; Reddy, M. S. Palladium(II)-Catalyzed Sequential Aminopalladation and Oxidative Coupling with Acetylenes/Enones: Synthesis of Newly Substituted Quinolines from 2-Aminophenyl Propargyl Alcohols. *Adv. Synth. Catal.* **2016**, *358*, 303−313.
(25) Ichake, S. S.; Konala, A.; Kavala, V.; Kuo, C. W.; Yao, C. F. Palladium-Catalyzed Tandem C-H Functionalization/Cyclization Strategy for the Synthesis of 5-Hydroxybenzofuran Derivatives. *Org. Lett.* **2017**, *19*, 54−57.
(26) (a) Li, J. X.; Li, C.; Ouyang, L.; Li, C. S.; Wu, W. Q.; Jiang, H. F. N-Heterocyclic carbene palladium-catalyzed cascade annulation/alkynylation of 2-alkynylanilines with terminal alkynes. *Org. Biomol. Chem.* **2017**, *15*, 7898−7908. (b) Li, J. X.; Hu, M.; Li, C. S.; Li, C.; Li, J. W.; Wu, W. Q.; Jiang, H. F. Palladium-Catalyzed Cascade Cyclization/Alkynylation and Alkenylation of Alkynone O-Methyloximes with Terminal Alkynes. *Adv. Synth. Catal.* **2018**, *360*, 2707−2719.
(27) Yan, Z. Y.; Tan, C. M.; Wang, X.; Li, F.; Gao, G. L.; Chen, X. M.; Wu, W. S.; Wang, J. J. Regioselective Synthesis of Substituted Imidate N-[1-Methyleneisobenzofuran-3(1H)-ylidene]benzenamines via Palladium-Catalyzed Tandem Heteroannulation of o-(1-Alkynyl)-benzamides with Iodobenzene. *Synlett* **2011**, *2011*, 1863−1870.
(28) Alvarez, R.; Vilar, U.; Madich, Y.; Aurrecoechea, J. M. On the regiochemical differences between Pd-catalyzed heterocyclization-allylation and -arylation reactions of alkynylbenzamides: preparation of 4-allyl-isochromen-1-imines and computational study. *Org. Biomol. Chem.* **2017**, *15*, 8594−8605.
(29) Álvarez, R.; Martínez, C.; Madich, Y.; Denis, J. G.; Aurrecoechea, J. M.; de Lera, Á. R. A General Synthesis of Alkenyl-Substituted Benzofurans, Indoles, and Isoquinolones by Cascade Palladium-Catalyzed Heterocyclization/Oxidative Heck Coupling. *Chem. - Eur. J.* **2010**, *16*, 12746−12753.
(30) Martínez, C.; Aurrecoechea, J. M.; Madich, Y.; Denis, J. G.; de Lera, Á. R.; Álvarez, R. Synthesis of Tetrahydrodibenzofuran and

DOI: 10.1021/acs.organomet.8b00519
Organometallics XXXX, XXX, XXX−XXX

Tetrahydrophenanthridinone Skeletons by Intramolecular Nucleopalladation/Oxidative Heck Cascades. *Eur. J. Org. Chem.* **2012**, *2012*, 99−106.

(31) Madich, Y.; Denis, J. G.; Ortega, A.; Martinez, C.; Matrane, A.; Belachemi, L.; de Lera, A. R.; Alvarez, R.; Aurrecoechea, J. M. A Practical Protocol for Three-Component, One-Pot, Stepwise Sonogashira-Heterocyclization-Heck Couplings. *Synthesis* **2013**, *45*, 2009−2017.

(32) Madich, Y.; Álvarez, R.; Aurrecoechea, J. M. Palladium-Catalyzed Regioselective 5-exo-O-Cyclization/Oxidative Heck Cascades from o-Alkynylbenzamides and Electron-Deficient Alkenes. *Eur. J. Org. Chem.* **2014**, *2014*, 6263−6271.

(33) Madich, Y.; Alvarez, R.; Aurrecoechea, J. M. Palladium-Catalyzed 6-endo-Selective Oxycyclization-Alkene Addition Cascades of ortho-Alkynylarylcarboxamides and alpha,beta-Unsaturated Carbonyl Compounds. *Eur. J. Org. Chem.* **2015**, *2015*, 6298−6305.

(34) Mancuso, R.; Ziccarelli, I.; Armentano, D.; Marino, N.; Giofrè, S. V.; Gabriele, B. Divergent Palladium Iodide Catalyzed Multicomponent Carbonylative Approaches to Functionalized Isoindolinone and Isobenzofuranimine Derivatives. *J. Org. Chem.* **2014**, *79*, 3506−3518.

(35) Yao, B.; Wang, Q.; Zhu, J. Palladium(II)-Catalyzed Cyclizative Cross-Coupling of ortho-Alkynylanilines with ortho-Alkynylbenzamides under Aerobic Conditions. *Angew. Chem., Int. Ed.* **2013**, *52*, 12992−12996.

(36) Yao, B.; Jaccoud, C.; Wang, Q.; Zhu, J. Synergistic Effect of Palladium and Copper Catalysts: Catalytic Cyclizative Dimerization of ortho-(1-Alkynyl)benzamides Leading to Axially Chiral 1,3-Butadienes. *Chem. - Eur. J.* **2012**, *18*, 5864−5868.

(37) For recent work that highlights the interest in isobenzofuranimines, see: (a) Schlemmer, C.; Andernach, L.; Schollmeyer, D.; Straub, B. F.; Opatz, T. Iodocyclization of o-Alkynylbenzamides Revisited: Formation of Isobenzofuran-1(3H)-imines and 1H-Isochromen-1-imines Instead of Lactams. *J. Org. Chem.* **2012**, *77*, 10118−10124. (b) Mehta, S.; Yao, T.; Larock, R. C. Regio- and Stereoselective Synthesis of Cyclic Imidates via Electrophilic Cyclization of 2-(1-Alkynyl)benzamides. A Correction. *J. Org. Chem.* **2012**, *77*, 10938−10944. (c) Bert, K.; Noel, T.; Kimpe, W.; Goeman, J. L.; Van der Eycken, J. Chiral imidate-ferrocenylphosphanes: synthesis and application as P,N-ligands in iridium(i)-catalyzed hydrogenation of unfunctionalized and poorly functionalized olefins. *Org. Biomol. Chem.* **2012**, *10*, 8539−8550. (d) Mehta, S.; Waldo, J. P.; Neuenswander, B.; Lushington, G. H.; Larock, R. C. Solution-Phase Parallel Synthesis of a Multisubstituted Cyclic Imidate Library. *ACS Comb. Sci.* **2013**, *15*, 247−254. (e) Araniti, F.; Mancuso, R.; Ziccarelli, I.; Sunseri, F.; Abenavoli, M. R.; Gabriele, B. 3-(Methoxycarbonylmethylene)isobenzofuran-1-imines as a New Class of Potential Herbicides. *Molecules* **2014**, *19*, 8261−8275. See also refs 27, 32, and 34−36.

(38) Grushin, V. V. Mixed phosphine-phosphine oxide ligands. *Chem. Rev.* **2004**, *104*, 1629−1662.

(39) For example, the formation of less stable, otherwise disfavored intermediates has been shown to be facilitated by air oxidation of PPh_3: Franzoni, I.; Yoon, H.; Garcia-Lopez, J. A.; Poblador-Bahamonde, A. I.; Lautens, M. Exploring the mechanism of the Pd-catalyzed spirocyclization reaction: a combined DFT and experimental study. *Chem. Sci.* **2018**, *9*, 1496−1509.

(40) Chinta, B. S.; Sanapa, H.; Vasikarla, K. P.; Baire, B. Highly regioselective, electrophile induced cyclizations of 2-(prop-1-ynyl)-benzamides. *Org. Biomol. Chem.* **2018**, *16*, 3947−3951.

(41) Balme, G.; Bouyssi, D.; Lomberget, T.; Monteiro, N. Cyclisations involving attack of carbo- and heteronucleophiles on carbon-carbon pi-bonds activated by organopalladium complexes. *Synthesis* **2003**, 2115−2134.

(42) Zeni, G.; Larock, R. C. Synthesis of heterocycles via palladium-catalyzed oxidative addition. *Chem. Rev.* **2006**, *106*, 4644−4680.

(43) Weigelt, M.; Becher, D.; Poetsch, E.; Bruhn, C.; Steinborn, D. On the oxidative addition of 1-halogenalk-1-ynes - Synthesis and structure of phenylalkynylalladium complexes. *Z. Anorg. Allg. Chem.* **1999**, *625*, 1542−1547.

(44) Wang, Z.-L.; Zhao, L.; Wang, M.-X. Construction of Caryl−Calkynyl Bond from Copper-Mediated Arene−Alkyne and Aryl Iodide−Alkyne Cross-Coupling Reactions: A Common Aryl-CuIII Intermediate in Arene C−H Activation and Castro−Stephens Reaction. *Org. Lett.* **2012**, *14*, 1472−1475.

(45) Urgoitia, G.; SanMartin, R.; Herrero, M. T.; Dominguez, E. Efficient copper-free aerobic alkyne homocoupling in polyethylene glycol. *Environ. Chem. Lett.* **2017**, *15*, 157−164.

(46) Sikk, L.; Tammiku-Taul, J.; Burk, P. Computational Study of Copper-Free Sonogashira Cross-Coupling Reaction. *Organometallics* **2011**, *30*, 5656−5664.

(47) For DMF as a weak donor ligand, see: (a) Ricci, A.; Angelucci, F.; Bassetti, M.; Lo Sterzo, C. Mechanism of the palladium-catalyzed metal-carbon bond formation. A dual pathway for the transmetalation step. *J. Am. Chem. Soc.* **2002**, *124*, 1060−1071. (b) Amatore, C.; Bahsoun, A. A.; Jutand, A.; Meyer, G.; Ntepe, A. N.; Ricard, L. Mechanism of the Stille reaction catalyzed by palladium ligated to arsine ligand: $PhPdI(AsPh_3)(DMF)$ is the species reacting with vinylstannane in DMF. *J. Am. Chem. Soc.* **2003**, *125*, 4212−4222. (c) Álvarez, R.; Nieto-Faza, O.; Silva-Lopez, C.; de Lera, A. R. Computational Characterization of a Complete Palladium-Catalyzed Cross-Coupling Process: The Associative Transmetalation in the Stille Reaction. *Org. Lett.* **2006**, *8*, 35−38. (d) Álvarez, R.; Nieto-Faza, O.; de Lera, A. R.; Cardenas, D. J. A density functional theory study of the Stille cross-coupling via associative transmetalation. The role of ligands and coordinating solvents. *Adv. Synth. Catal.* **2007**, *349*, 887−906. (e) Álvarez, R.; Pérez, M.; Nieto-Faza, O.; de Lera, A. R. Associative Transmetalation in the Stille Cross-Coupling Reaction to Form Dienes: Theoretical Insights into the Open Pathway. *Organometallics* **2008**, *27*, 3378−3389.

(48) Ahlquist, M.; Fabrizi, G.; Cacchi, S.; Norrby, P. O. Palladium(0) alkyne complexes as active species: a DFT investigation. *Chem. Commun.* **2005**, 4196−4198.

(49) Graphical representations have been generated using ChemCraft (graphical software for visualization of quantum chemistry computations): https://www.chemcraftprog.com.

(50) Sashida, H.; Kawamukai, A. Palladium-catalyzed intramolecular cyclization of 2-ethynylbenzoic acids and 2-ethynylbenzamides. Preparation of isocoumarins and isoquinolin-1-ones. *Synthesis* **1999**, *1999*, 1145−1148.

(51) Zhang, S. W.; Kaneko, T.; Yoneda, E.; Sugioka, T.; Takahashi, S. Rhodium-catalyzed cyclic carbonylation of 2-phenylethynylbenzamide under water-gas shift reaction conditions. *Inorg. Chim. Acta* **1999**, *296*, 195−203.

(52) Liu, G. N.; Zhou, Y.; Ye, D. J.; Zhang, D. Y.; Ding, X.; Jiang, H. L.; Liu, H. Silver-Catalyzed Intramolecular Cyclization of o-(1-Alkynyl)benzamides: Efficient Synthesis of (1H)-Isochromen-1-imines. *Adv. Synth. Catal.* **2009**, *351*, 2605−2610.

(53) (a) Ditchfield, R.; Hehre, W. J.; Pople, J. A. Self-Consistent Molecular-Orbital Methods. IX. An Extended Gaussian-Type Basis for Molecular-Orbital Studies of Organic Molecules. *J. Chem. Phys.* **1971**, *54*, 724−728. (b) Hehre, W. J.; Ditchfield, R.; Pople, J. A. Self-Consistent Molecular Orbital Methods. XII. Further Extensions of Gaussian-Type Basis Sets for Use in Molecular Orbital Studies of Organic Molecules. *J. Chem. Phys.* **1972**, *56*, 2257−2261.

(54) Frisch, M. J.; Trucks, G. W.; Schlegel, H. B.; Scuseria, G. E.; Robb, M. A.; Cheeseman, J. R.; Scalmani, G.; Barone, V.; Mennucci, B.; Petersson, G. A.; Nakatsuji, H.; Caricato, M.; Li, X.; Hratchian, H. P.; Izmaylov, A. F.; Bloino, J.; Zheng, G.; Sonnenberg, J. L.; Hada, M.; Ehara, M.; Toyota, K.; Fukuda, R.; Hasegawa, J.; Ishida, M.; Nakajima, T.; Honda, Y.; Kitao, O.; Nakai, H.; Vreven, T.; Montgomery, J. A., Jr.; Peralta, J. E.; Ogliaro, F.; Bearpark, M.; Heyd, J. J.; Brothers, E.; Kudin, K. N.; Staroverov, V. N.; Kobayashi, R.; Normand, J.; Raghavachari, K.; Rendell, A.; Burant, J. C.; Iyengar, S. S.; Tomasi, J.; Cossi, M.; Rega, N.; Millam, J. M.; Klene, M.; Knox, J. E.; Cross, J. B.; Bakken, V.; Adamo, C.; Jaramillo, J.; Gomperts, R.; Stratmann, R. E.; Yazyev, O.; Austin, A. J.; Cammi, R.; Pomelli, C.;

DOI: 10.1021/acs.organomet.8b00519
Organometallics XXXX, XXX, XXX−XXX

Ochterski, J. W.; Martin, R. L.; Morokuma, K.; Zakrzewski, V. G.; Voth, G. A.; Salvador, P.; Dannenberg, J. J.; Dapprich, S.; Daniels, A. D.; Farkas, Ö.; Foresman, J. B.; Ortiz, J. V.; Cioslowski, J.; Fox, D. J. *Gaussian 09, Revision B.01*; Gaussian, Inc., Wallingford, CT, 2009.

(55) (a) Hay, P. J.; Wadt, W. R. Ab initio effective core potentials for molecular calculations. Potentials for the transition metal atoms Sc to Hg. *J. Chem. Phys.* **1985**, *82*, 270−283. (b) Wadt, W. R.; Hay, P. J. Ab initio effective core potentials for molecular calculations. Potentials for main group elements Na to Bi. *J. Chem. Phys.* **1985**, *82*, 284−298. (c) Hay, P. J.; Wadt, W. R. Ab initio effective core potentials for molecular calculations. Potentials for K to Au including the outermost core orbitals. *J. Chem. Phys.* **1985**, *82*, 299−310.

(56) (a) Foster, J. P.; Weinhold, F. Natural hybrid orbitals. *J. Am. Chem. Soc.* **1980**, *102*, 7211−7218. (b) Reed, A. E.; Weinhold, F. Natural bond orbital analysis of near-Hartree−Fock water dimer. *J. Chem. Phys.* **1983**, *78*, 4066−4073. (c) Reed, A. E.; Weinstock, R. B.; Weinhold, F. Natural population analysis. *J. Chem. Phys.* **1985**, *83*, 735−746. (d) Reed, A. E.; Weinhold, F. Natural localized molecular orbitals. *J. Chem. Phys.* **1985**, *83*, 1736−1740.

(57) Marenich, A. V.; Cramer, C. J.; Truhlar, D. G. Universal Solvation Model Based on Solute Electron Density and on a Continuum Model of the Solvent Defined by the Bulk Dielectric Constant and Atomic Surface Tensions. *J. Phys. Chem. B* **2009**, *113*, 6378−6396.

DOI: 10.1021/acs.organomet.8b00519
Organometallics XXXX, XXX, XXX−XXX